2018

Assessing Exposure to Occupants in an Indoor Space Due to Expirated Aerosols: Application of Computational Fluid Dynamics

Firoza Binte Omar
University of South Carolina

Assessing Exposure to Occupants in an Indoor Space Due to Expirated Aerosols: Application of Computational Fluid Dynamics

by

Firoza Binte Omar

Bachelor of Architecture
Bangladesh University of Engineering and Technology, 2009

Submitted in Partial Fulfillment of the Requirements

for the Degree of Master of Science in

Civil Engineering

College of Engineering and Computing

University of South Carolina

2018

Accepted by:

Shamia Hoque, Director of Thesis

Enrica Viparelli, Reader

Jamil A. Khan, Reader

Cheryl L. Addy, Vice Provost and Dean of the Graduate School

Dedication

To my mom, 'Shellyna Arzuband Banu' and my dad, 'Omar Faroque', who have sacrificed a lot and inspired me to pursue my dreams even at the most difficult times. And also to my beloved husband, 'Dr. Nowrin Hasan Chamok' for his love and undeniable support and motivation.

Acknowledgments

I would like to express my sincere gratitude to my supervisor Dr. Shamia Hoque for her continuous support throughout my masters journey. I feel privileged to have such a mentor who has always guided me with her knowledge, time, motivation, and career advices. Her precious words during the tough times in my pregnancy has given me the strength and encouragement to stay on. I am also gratefully indebted to my thesis committee members: Dr. Enrica Viparelli and Prof. Jamil A. Khan for their valuable comments and advices to improve this thesis.

I would like to extend my sincerest appreciation to my parents, Shellyna Arzumand Banu and Omar Faroque, and my siblings-specially my elder brother Abu Shoaib Ibne Omar for his selfless contributions, and my in-laws who have been constant sources of encouragement throughout this journey. I would also like to acknowledge my friends and relatives in Bangladesh for their unconditional love and caring.

I would like to extend my gratitude to my friends and members of Bangladeshi community in Columbia and in California, specially to Dr. Fazle Rabbi, Dr. Shamaita Shithi Shetu, Fatema J Zahan, Rowshan Ara Rima, and Sayeeda Rayhan who provided me all the supports I needed to cope with a new environment far away from home. My heartiest gratitude to Dr.Nazratun Monalisa who took care of me as an elder sister when I needed most.

My cordial thanks go to my labmate Dahae Seong for her help specially while working offsite, my collegues: Dr. Liang Li, Ife Louwapo, Malu Devadasan, for their selfless assistance and suggestions. I am thankful to our office staff members

Ammarell Karen, Patrick Blake, Brian Hull and Kate for all the technical and formal supports specially at the time working offsite.

This thesis could not be possible without the constant encouragement, assistance, and sacrifices of my beloved husband, Dr. Nowrin Hasan Chamok. He was always there for me and never lost hope on me even in my toughest and most vulnerable times. I have become a mom for the first time during this thesis. My precious daughter Bineeta Bornomala is always an inspiration to me.

Abstract

Indoor environment is an important issue for the well-being of the society. In the United States more than 90% people spend their time indoor, indoor air pollution is more culpable than the pollution outside air. Two third of US businesses lose more than $100,000 per year due to workplace related illness. The trend of sharing the work space has an impact on total sick leaves in a company. Infectious particles released by a flu sufferer's sneezing, coughing or even laughing can be a vital source. A thorough analysis on infectious particles' transmission and air flow of the space can provide an effective solution to design and control of healthy indoor environment. The interior design i.e. furniture orientation, the air inlet and outlet locations and safe space distribution between the working zones can play a significant role in determining the most effective, energy efficient and healthy indoor layout.

In this study, a detailed computational fluid dynamics (CFD) simulations applying an Eulerian - Langrangian framework is performed to investigate the spread of infectious particles after sneezing in a ventilated office space and the length of time they reside in the breathing zone thus estimating the possibility of infection of another occupant. The observations from 18 distinct cases, varying ventilation rate (ACH 3, 5, and 7), ventilation pattern and furniture condition (with a partition wall only, and with partition wall and desk) demonstrate that only ACH increase cannot be a solution to reduce the risk of infection spreading, the ventilation pattern has a significant role and it defers with the room furniture conditions. Two types of ventilation pattern- mixed ventilation (MV) and displacement ventilation (DV) are assessed. MV pattern has been sub-divided into ceiling (inlet-outlet in the ceiling)

and cross (inlet-outlet in opposite walls) ventilation.

Increasing ACH from 3 to 7 reduce ≈45-50% more dead-zones in the room. At higher ACH, ceiling ventilation and displacement ventilation are more effective in removal of particles from the room as well as from the breathing zone. Moreover, the presence and absence of the furniture is an important factor to decide the ventilation rate and pattern to ensure healthier indoor space. With ACH 7, ceiling ventilation and MV-cross ventilations offers most favorable condition in a room with partition wall only and in a room with a partition wall and desk respectively. At lower ACH, MV-cross ventilation was found to be the most inefficient scheme for both room conditions. A preliminary study with multiple sized particles reveals particle number in the breathing zone did not vary substantially over time. The cost analysis shows that the monetary value to increase the ventilation rate is reasonable comparing to the annual loss from the inefficiency of the sick employees.

Table of Contents

List of Tables

List of Figures

Chapter 1

Introduction

1.1 Background and Motivation

In present-days, human lives and activities are centered around built environment and indoor spaces. In the United States, people spend around 90% of their time indoors (Klepeis et al., 2001). Since most individuals daily activities take place inside, the atmosphere of indoor space has a major impact on the health and safety of most of the population. It has been reported that indoor air can have 2 to 5 times higher pollutant concentration than typical outdoor air EPA (2003) and it can have more damaging effects on health than pollution in the air outside. It is, therefore, very important to evaluate the indoor air quality which is a complex interaction of several factors such as the room geometry, air change rate, ventilation pattern, room organization etc. Furthermore, to assess the health risk, it is crucial to investigate the behavior and trajectories of the infectious particles present inside the room.

Generally, these infectious particles can be modeled as 'aerosols' that are suspensions in air (or in a gas) consisting of small solid or liquid particles that remain airborne for a prolonged period because of their low settling velocity. Aerosol droplets are generated and released during speech, coughing, sneezing or even while laughing (Morawska, 2006). This often leads to aerosol transmission of diseases such as common cold, influenza, anthrax, tuberculosis etc. These diseases can affect the overall productivity of an work space significantly. According to a review by Keech and Beardsworth (2008), each staff diagnosed with flu loses 4 days on average in form of

sick days. The monetary impact cannot be ignored too, as two thirds of U.S. businesses admit that their company lose more than $100,000 per year due to workplace related illnesses (Staples, 2016). One aspect of controlling the spread of diseases is to establish some hygienic human behaviors such as covering mouth while sneezing and coughing, staying away from public when affected, sanitizing hand after sneezing, or after touching places where others touch frequently such as door handles, bathroom faucets, vending machine keys etc. From a management perspective, it is hard to administer these health codes. Study shows that 25% people do not cover their mouth while coughing and sneezing (Liu and Novoselac, 2014). A study by (Staples, 2016) showed while four fifths are worried of getting sick when their co-workers come into work with flu, another 80% responded that they went to office anyway when contagious due to several reasons.

This brings us another perspective of controlling the spread of illness: by controlling environmental parameters like HVAC system, ACH, furniture layout and ventilation pattern. Aerosol or particle transport and distribution are highly associated with airflow pattern and turbulence. There is a strong and sufficient evidence to establish the relationship between ventilation, airflow pattern in building and the spread of infectious diseases (Liu and Novoselac, 2014). Low ventilation rates (<25 liter/sec per person) have been linked with more cases of Sick Building Syndrome (SBS), a situation where occupants suffer from headaches and respiratory problems (Pejtersen et al., 2011; Wargocki et al., 2000). A similar study shows that at schools, low ventilation rates had a negative impact on school absence and respiratory illness (Sundell et al., 2011). The efficiency of a ventilation system depends on particle removal or supplying fresh air to the breathing zone (Cao et al., 2014). Air flow pattern and aerosol transport in the breathing zone can have significant influence on disease transmission and cross infection in spaces with multiple occupants.

Besides the HVAC system, indoor space design and organization play a role in

ensuring a healthy environment and minimizing exposure to the residents. It has been shown that, compared to cellular offices, occupants in two persons offices had 50% and in open-plan offices (>6 persons) had 62% more days of sickness absence (Sundell et al., 2011). Now, the variables in a space can be identified mostly as the type of the space (e.g. restaurant, workshop, office, mall area etc.), number of people sharing the space, number of sick people, equipment and furniture in the room.

To design an efficient well-ventilated indoor space and to understand the particle behavior properly, it is very important to examine the simultaneous interaction among the key factors such as air change rate, ventilation patterns, room geometry and organization, particle size etc. In this thesis, we investigated the air flow pattern and air quality of an indoor room with a partition wall. Also, we studied the fates of particles exhaled during uncovered sneeze or cough with three air change rates, three different ventilation patterns, two room conditions, and multiple particle sizes.

1.2 Literature Review

The investigation of the dispersion pattern of aerosol particles needs to be conducted with reasonable accuracy to provide information to decision makers and designers to ensure healthy environment. With the increased computational speed and more knowledge of the system to build accurate numerical experiments, Computational Fluid Dynamics (CFD) has become very popular to realize such complex system and there has been a growing interest among researchers to model the scenarios precisely. Following is a brief summary of the works that are relevant to this thesis.

1.2.1 Ventilation as a Part of HVAC System

Controlling the outdoor air flow or designing the ventilation pattern are parts of the HVAC system of a building. The American Society of Heating, Refrigerating and Air-Conditioning Engineers (ASHRAE) is the largest organization who standardize

HVAC system. ASHRAE Standard 62.1 recommends that in an office space the minimum ventilation rate in the breathing zone should be 17 cubic ft/min/per person (ASHRAE, 2016). As modeling the entire HVAC system is extremely complex often different strategies are followed to analyze it. A comprehensive review by Afroz et al. (2018) classified these modelling into three categories: mathematical, empirical and hybrid. In the mathematical modelling approach, simulations are performed using a set of equations based on laws of physics such as mass balance, heat transfer etc. This method is usually used in design phase to predict the performance of an HVAC system. The empirical or data driven modelling is done after the installation of an HVAC system, to improve the existing system. The hybrid models combine both approaches- they use both simulation and measurement data to predict or improve HVAC systems.

1.2.2 Effect of Ventilation Pattern and Particle Size on Particle Fate

Lu et al. (1996) and Lu and Howarth (1996) employed CFD models to investigate air flow, particle transport, and deposition in a two-zone room where they inferred that particle properties, ventilation settings, and airflow patterns were the governing factors of particle behavior. But they used only a single type of ventilation scheme namely the mixed cross ventilation and the room was not furnished. Similar numerical techniques were used by Chang et al. (2006) to study particle removal behavior in a multi- room building which had cross-flow displacement ventilation. He concluded that the smaller sized particles have lower removal efficiency and higher sensitivity to airflow pattern than the larger ones (Fig. 1.1).

The experimental findings from Thatcher et al. (2002) confirmed that although particle size have a large effect on deposition loss rates, particle fate is highly dependent on room furnishing and air speed too. They studied the effect of room furnishings on particle deposition rates using three furnishing levels and four air flow conditions.

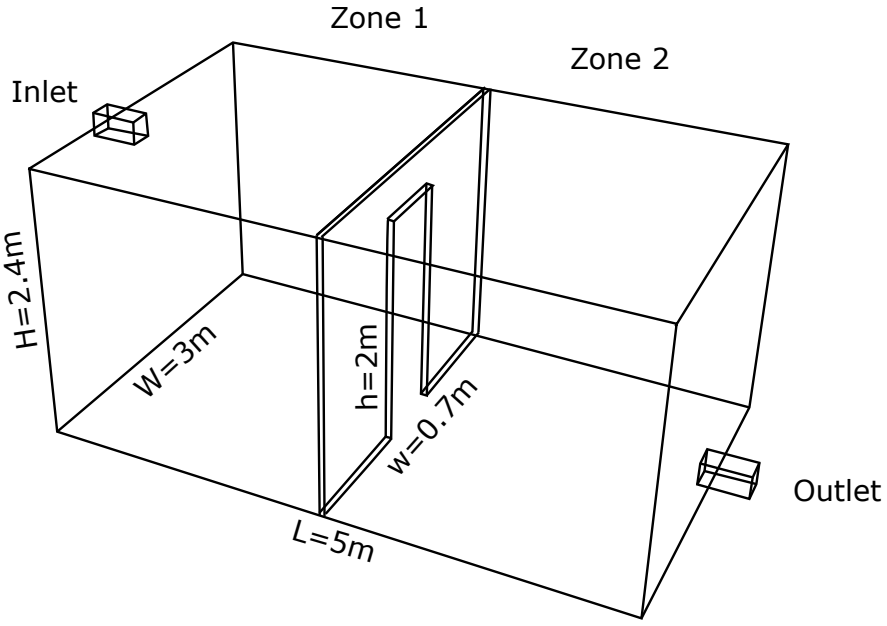

Figure 1.1 The room geometry configuration for the simulations done by Lu et al (1996).

To study the effect of ventilation patterns have been a point of interest for a long time (Ansaripour et al., 2016; Canha et al., 2017; Gao and Niu, 2007; Hathway et al., 2011; Liu et al., 2017; Quang et al., 2013; Zhou et al., 2017).

Among them Gao and Niu (2007) used CFD techniques to model particle dispersion and deposition in indoor space where, studying three ventilation types (mixing ventilation, displacement ventilation, and under-floor air distribution), they showed that the ventilation type and particle size have the largest impact on particle fate. They also established an inverse relationship between particle size and human exposure.

Hathway et al. (2011) conducted CFD simulations to inspect aerial transport of infectious particles in an equipped hospital room with two different types of ventilation and three different types of air change rates. He emphasized how accurate positioning of particle source might affect fates of particles.

Very recently Ansaripour et al. (2016) performed numerical analysis to study par-

ticle transport in a room with a seated manikin where they observed effects of different ventilation configurations on the breathing zone concentration. They recommended mixing ventilation system to ensure the lowest mean particle concentration in the breathing zone but the study was done with a constant air change rate.

1.2.3 Effect of Air Change Rates

Air change rate can have a big impact on particle transportation as shown by Faulkner et al. (2015), who generated empirical data to feed CFD simulations. They showed that for small particles (1.9 um), average concentration was in inverse linear relation with ventilation rate. This finding is in accordance with Knudsen et al. (2017) who, having investigated fungal spore particles, concluded that increasing air flow rate resulted in lower particle concentrations. However, Putra and Rahman (2017) studied an office building to examine the effect of ventilation rate on indoor air quality and they indicated that increasing ventilation rate alone might not be the most effective policy for improving indoor air quality. The geometry configuration that was used by Putra and Rahman (2017) is shown in Fig. 1.2.

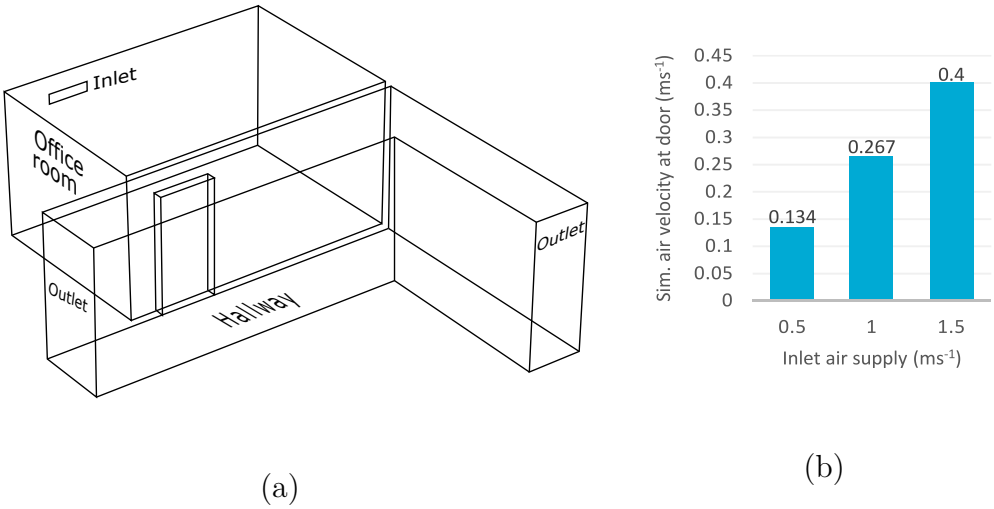

(a) (b)

Figure 1.2 (a) The geometry configuration and (b) air flow result from the study done by Putra and Rahman (2017).

It has been reported that increasing air change rate by 1 can cause a $150-$250 increase in HVAC cost per year (Memarzadeh and Xu, 2012). As increasing air change rate demands for more expensive HVAC system in terms of money and energy usage, cost effectiveness plays an important role for choosing the optimum solution (Wu et al., 2018).

1.2.4 Modeling of Respiratory Particles

To study the transmission of particles released during sneezing or coughing, it is important to know how to model the droplets accurately. Some key parameters for this modeling are number, size, and velocity of the particles during release. Substantial research have been done to find these factors.

Cole and Cook (1998) found that about 40,000 droplets are released during sneeze. Lindsley et al. (2012) reported that the number of droplets released during a single cough ranges from 900 to 302,200. There are some differences regarding the particle size across the literature but the numbers fall in the same estimate region. Yang et al. (2007) observed that the diameter of the cough droplets ranges from 0.62-15.9 μm, where the range is Lindsley et al. (2012) 0.35 to 10 μm. Here, an important observation was presented by Nicas et al. (2005) who showed that emitted droplets with diameters < 20 μm instantenously evaporate to 50% of their initial diameter.

Zhu et al. (2006) conducted a study to determine the velocity of the cough particle dusring release where the peak cough velocity was found to be in the range of 6 to 22 m/s with a mean of 11.2 m/s.

1.3 Objective

The objectives of the current work were the following.

(a) Identify the vital parameters which are influential in particle transport and fate in the indoor space

(b) Investigate the air flow pattern and particle behavior with different combinations of the parameters. The investigation was done with two dimensional CFD simulations.

(c) Analyze how the different parameters influence air quality in the room as well as in the breathing zone.

(d) Evaluate the data and suggest the preferable ventilation pattern and rate for a specific room condition.

In short, the main goal was to determine the optimum room condition for safe and healthy environment based on investigating the interplay between several key parameters of indoor space.

1.4 Thesis Outline

The thesis is organized into five chapters. Chapter 1 describes the background and objective of the study. Review of several literatures and objectives of the study is also presented in this chapter. Chapter 2 depicts the problem scenario of the study. Chapter 3 presents the methodology of the research work. The underlying theories, mathematical model of computational fluid dynamics, and the simulation set up are described in detail in this chapter. The air flow condition and the particles fate and transport under different conditions are analyzed and discussed the findings based on the simulation results in the Chapter 4. Chapter 5 summarizes the conclusion and recommendations for future research directions.

Chapter 2

Problem Setup

The problem was set and simulated as a '2D domain', with the exhale and inhale zone separated by a partition wall. Figure 2.1 is representative of the domain of a base case scenario with the pertinent variables listed in Table 2.1. Here, w_I is the width of the inlet,w_o is the width of the outlet, h_I is the height of the inlet from the floor, h_O is the height of the outlet from the floor, D_{wp} is the distance between the wall (left) and the partition wall, and D_{wo} is the distance between the wall (left) and first obstruction. The variables were chosen in a manner to ensure that the impact of the indoor configurations on particle transport can be tested. The table adds a third column where dimensionless groups or ratios of the variables have been included.

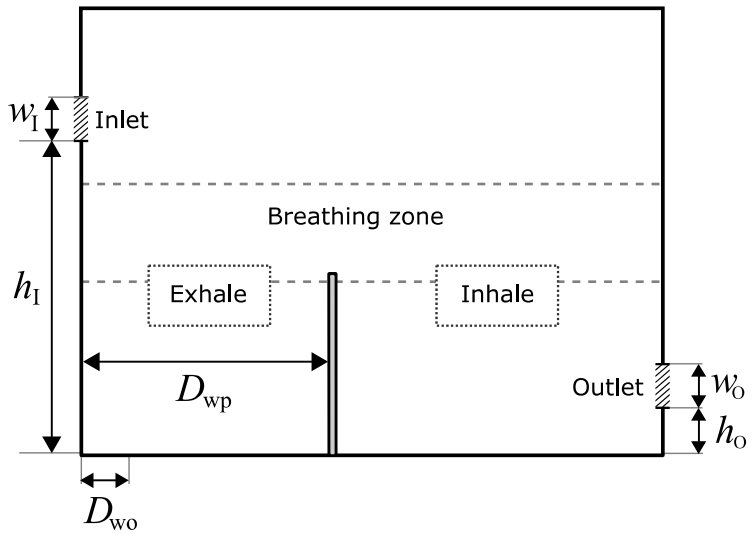

Figure 2.1 Base case scenario.

Three different ventilation types and two interior arrangements are considered.

Table 2.1 Dimensionless groups describing the problem scenario.

Variable	Symbol	Dimensionless ratio
Height of the inlet from the bottom of the domain	h_I	$\frac{h_I}{h_O}$
Height of the outlet from the bottom of the domain	h_O	
In exhale zone, distance between wall and partition	D_{wp}	$\frac{D_{wp}}{D_{wo}}$
In inhale zone, distance between wall and first obstruction	D_{wo}	

Table 2.2 lists the ventilation types. The three types of ventilation pattern are (1) inlet and outlet of the domain located at the top, i.e., the ratio of the height of the inlet (h_I) to the height of the outlet (h_O) is 1, (2) inlet and outlet located opposite walls with the inlet positioned higher than the outlet hence $h_I/h_O > 1$ and (3) the inlet is located on the opposite wall positioned lower than the outlet, $h_I/h_O < 1$.

In the exhale zone the distance from the wall to the partition is D_{wp} and the distance from the wall to the first obstruction is D_{wo}. For the scenarios with desks $D_{wo}/D_{wp} < 1$ and in the cases without desks $D_{wo}/D_{wp} = 1$. For each ventilation type three air changes per hour (ACH), 3, 5, and 7 were considered. The recommended ACH for office spaces is 4-10 ACH (ASHRAE 62.1, 62.2). For public and private offices the common practice is to maintain 3 and 4 ACH respectively (Toolbox, 2005). In this study ACH of 3, 5, and 7 were chosen to assess situations as those are representative of common scenario. For all three ventilation patterns, it was assumed that there is one inlet and one outlet in the room.

We considered two different interior configurations: a room with a partition wall and a room with the partition wall and two working desks. These can be considered representative of a workspace shared by two occupants. For both scenarios, a 1.22 m (4 ft) high partition wall is present. The room is 4.88 m (16 ft.) in long with a height

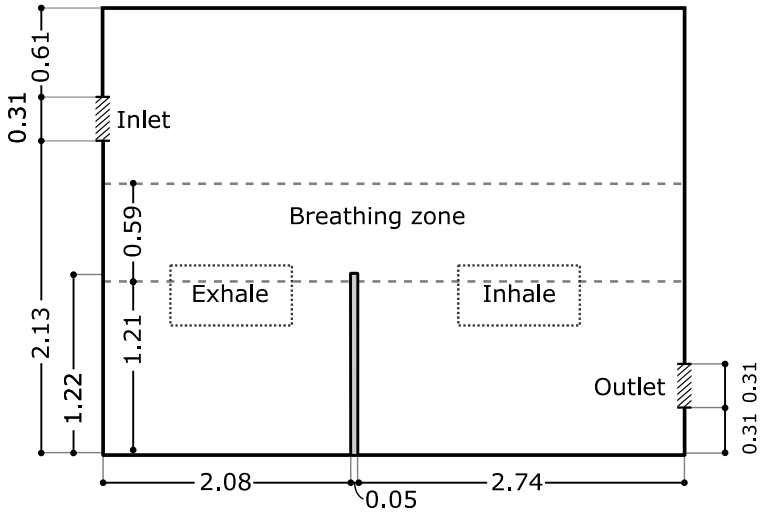

Figure 2.2 Room geometry without desk (dimensions in 'm').

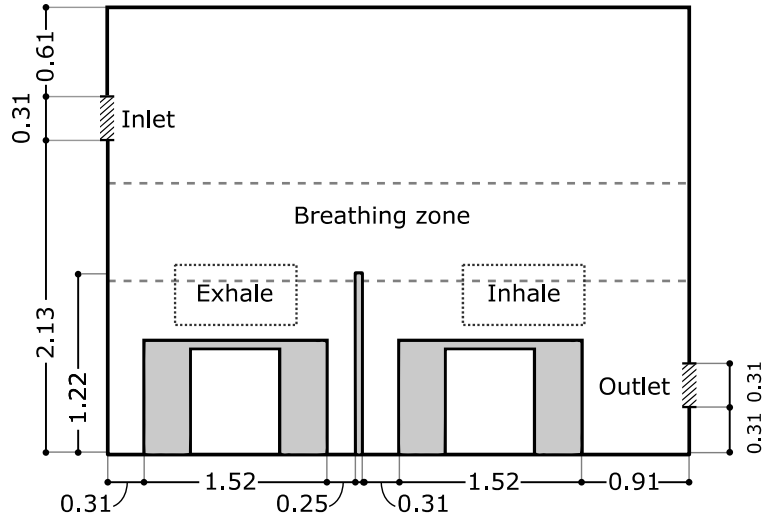

Figure 2.3 Room geometry with desks (dimensions in 'm').

of 3.05 m (10 ft.). Figure 2.2 and Figure 2.3 shows the detailed dimensions of the room geometry for Mixed Ventilation-Cross type. In Figure 2.2, the geometry is set for a room with a 4 ft partition wall, and in Figure 2.3, a space with a partition all and two working desks are shown. The working desk maintains the standard dimensions having a length of 1.52 m (5 ft.) and a height of 0.76 m (30 in). The width of both

Table 2.2 Ventilation Patterns.

Ventilation type	Inlet and outlet location
Mixed Ventilation (MV) - Ceiling	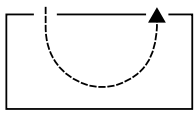
Mixed Ventilation (MV) - Cross	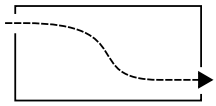
Displacement Ventilation (DV) - Cross	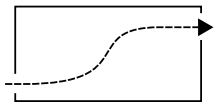

inlet and outlet is 0.305 m (1 ft.). For the mixed ceiling ventilation (MV-Ceiling) the inlet and outlet both are on the ceiling at 0.61 m (2 ft.) from the side wall. In mixed cross ventilation (MV-Cross), the inlet is on the side wall at 0.61 m (2 ft.) below from the ceiling and the outlet is on the opposite side walls at 0.305 m (1 ft.) from the floor level. For displacement cross ventilation (DV-Cross) the inlet is 0.305 m (1 ft.) from the floor level and the outlet is on the opposite wall 0.61 m (2ft.) below the ceiling level. Inlet flow velocity was adjusted to obtain 3, 5, 7 Air Change per Hour (ACH). With three choices for ACH, three ventilation patterns and two room conditions we have a combination of 18 scenarios. The details are given in Table 2.3.

In this study we have investigated the particles generated from a sneeze directly to the indoor area. It is assumed that one employee or occupant sneezes (exhale location) without covering his or her mouth and he/she is considered to be the source of particles released in the domain. Also, we have assumed that there is another employee or occupant working or staying on the other side of the partition wall who is in risk of inhaling the sneezed particles (inhale location). The breathing zone has been identified according to Occupational Safety and Health Administration (OSHA, 2016) which is the height between 1.21 m and 1.80 m from the floor level accounting for both sitting and standing positions.

Table 2.3 Simulation details.

Case no.	h_1/h_o	ACH	D_{wo}/D_{wp}	Schematic
1	1	3	1	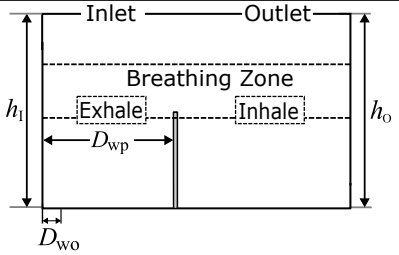
2	1	5	1	
3	1	7	1	
4	1	3	<1	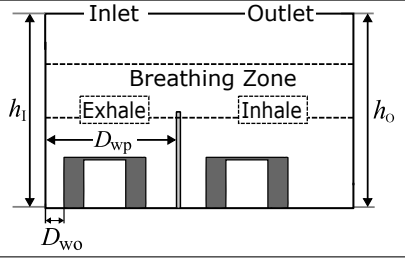
5	1	5	<1	
6	1	7	<1	
7	>1	3	1	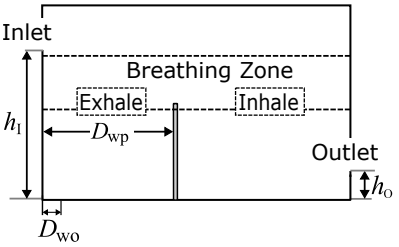
8	>1	5	1	
9	>1	7	1	
10	>1	3	<1	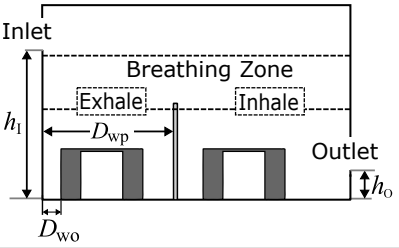
11	>1	5	<1	
12	>1	7	<1	
13	<1	3	1	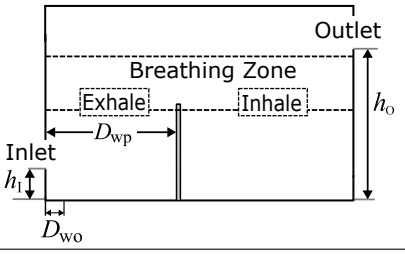
14	<1	5	1	
15	<1	7	1	
16	<1	3	<1	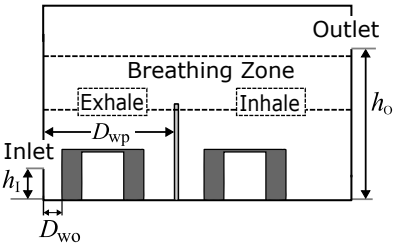
17	<1	5	<1	
18	<1	7	<1	

The ‘exhalation zone’ is the region where the residing occupant sneezes. The ‘inhalation zone’ is identified as the region of the breathing zone where the second office occupant is located. The two regions are separated by the partition wall.

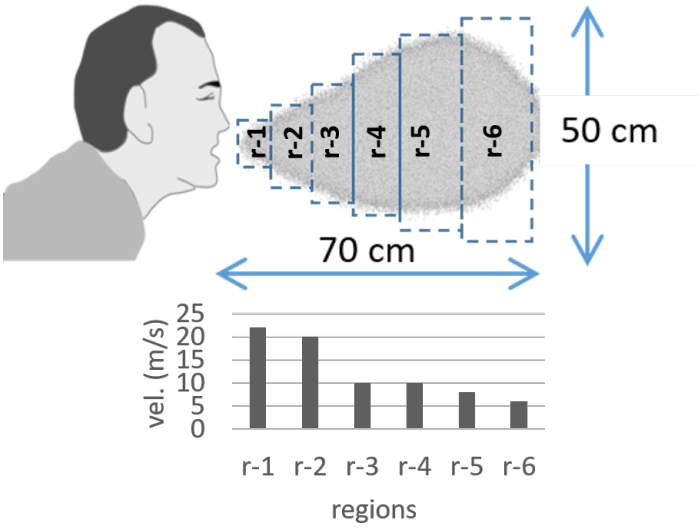

Figure 2.4 Sneeze model.

Figure 2.4 is a schematic of the simulation of a sneeze. The domain of the sneeze is of 0.7 m in length and 0.5 m in height. The area is divided into six segments where aerosols are injected randomly with a velocity range of 6-22 m/s (Zhu et al., 2006). Average range of particle that released through cough is 900 to 302,200 (Liu and Novoselac, 2014). For the simulation, the number is selected to be 150,000 (mid-range) and distributed in the six regions and high number of particles are sprayed at the point of release. It has been observed that the coughed particles have a wide range of sizes, with different transport characteristics. The size range is observed as 0.35 to 10 μm by Lindsley et al. (2012) also observed that coughed particles have a size range of 0.35 to 10 μm and 0.62-15.9 mm with nuclei sizes of 0.58-5.42 μm by Yang et al. (2007). The emitted droplets with diameters $<$20 μm rapidly evaporate to 50% of their initial diameter Nicas et al. (2005). For the simulation the size of the particles

chosen is from the mid-range. In this study, the particle size is assumed 7 μm for all cases. To simulate the high momentum at the point of release and the subsequent loss of energy, it is assumed that the particles released closer to the source have the maximum velocity and as the distance increases the particle velocity reduces.

Chapter 3

Computational Fluid Dynamics Model Development

3.1 Introduction

Computational fluid dynamics (CFD) is a mathematical modeling approach in which the Navier-Stokes equations are solved to calculate the fluid parameters. The governing equations of fluid flow are partial differential equations; when discretized on grids, they transform into algebraic equations which can be solved by a finite-difference/finite-volume algorithm (Basarir, 2009). In the present study, the numerical simulations were conducted using the commercial code CFD-ACE+ (ESI, 2014). The simulations were executed an IBM desktop with a processor of Intel (R) Core (TM) i7-4790 @ 3.60 GHz, 16.0 RAM and of 64-bit operating system, and a cluster. CFD analysis took place in three stages:

- First a pre-processing application (present study: CFD-GEOM) was used to draw the model geometry. The boundaries (walls, inlet, outlet, furniture) and the volume (fluid, solid) were also defined in this step. After that, the fluid domain was divided with non-uniform structured grids.

- The model was then imported in CFD-ACE-GUI to solve the flow field equations in grid points. After developing a pseudo steady initial condition, particles were released in the domain.

- The CFD solver CFD-ACE would generate the flow field data and spray data at

each grid point after solving the appropriate governing equations. After the data was generated by the solver, it was exported to a data processor (in the present work, CFD-VIEW) to generate line plots, flow variable contours, and particle animations. This data was then exported to other software such as Excel and Matlab for better visualizations and comparisons with other scenarios.

3.2 Mathematical Model Formulation

The CFD model is based on the Eulerian Lagrangian framework. It comprises of submodules for calculating the air flow and particle trajectories.

3.2.1 Airflow Model

For airflow simulation 'Reynolds Averaged Navier-Stokes' (RANS) modeling and 'Large Eddy Simulation' (LES) schemes were applied. The air flow was treated as a turbulent flow characterized by eddies having a long period of time and length modeled by Large Eddy Simulation (LES).

The mathematical complexity of LES simulation lies between direct numerical simulation and Reynolds Averaged Navier Stokes (N-S). As a technique, LES is a compromise between RANS and DNS. In DNS the solution is obtained by computing all the turbulence scales using the time dependent Navier-Stokes equations. Very fine spatial/temporal grids are required for this scheme. Therefore, it requires extensive computing power with fast processors and large memory blocks to simulate airflow characteristics in an indoor structure (Piomelli, 1999). In comparison, the RANS modeling scheme focuses on generating the mean velocity field by applying different turbulent models. As this scheme does not generate instantaneous velocity field it results in lower accuracy in the computation of particle dispersion. The LES model offers a better scenario in this situation for it generates the instantaneous flow information which is critical to particle transport simulation (Tian et al., 2007).

The LES scheme works by utilizing a filter to remove small-scale turbulence from the Navier-Stokes equations and then evaluating the small scales with a separate model. Usually the filter size is selected to be equal to the smallest grid size. Large scales motions are computed by solving these modified Navier-Stokes equations which eventually provides information for most of the energy transport and momentum. In contrast, information regarding the large eddies can be obtained from the small scales of the sub grid models.

The Navier-Stokes Equations for incompressible flow of a Newtonian fluid are given by: :

$$\frac{\partial u_i}{\partial x_i} = 0 \tag{3.1}$$

$$\frac{\partial \bar{u}_i}{\partial t} + \frac{\partial}{\partial x_i}(\bar{u}_i \bar{u}_j) = -\frac{1}{\rho}\frac{\partial \bar{p}}{\partial x_i} - \frac{\partial \tau_{ij}}{\partial x_j} + \nu_t \frac{\partial^2 \bar{u}_j}{\partial x_i \partial x_j} \tag{3.2}$$

In the equations (3.1) and (3.2) u and p represents turbulent velocity and pressure respectively. The effect of the small scales can be determined by evaluating the subgrid-scale (SGS) stress term, τ_{ij} (Piomelli, 1999) applying equation (3.3), where ν_t is the turbulent eddy viscosity and $\bar{S}_{ij}$ is the rate of strain tensor.

$$\tau_{ij} - \frac{\tau_{kk}\delta_{ij}}{3} = 2\nu_t \bar{S}_{ij} \tag{3.3}$$

The small scales are generally more isotropic than their large counterparts. Straightforward algebraic expressions can be used to model those without significantly compromising the accuracy of physics and many flow situations can me modelled using this scheme (Piomelli, 1999).

The Smagorinsky model is the most commonly used subgrid-stress model which is an eddy viscosity model (Piomelli, 1999). The subgrid-scale stresses are related to the large-scale strain rate tensor by Equation (3.4).

$$\bar{S}_{ij} = \frac{1}{2}\left(\frac{\partial u_i}{\partial x_j} + \frac{\partial u_j}{\partial x_j}\right) \tag{3.4}$$

The eddy viscosity, ν_t is obtained from the algebraic model (Equations 3.5 and 3.6), where Δ=grid size and C_s = Smagorinsky constant.

$$\nu_t = C_s \Delta^2 |\bar{S}| \bar{S}_{ij} \tag{3.5}$$

$$|\bar{S}| = \left(2\bar{S}_{ij}\bar{S}_{ij}\right)^{\frac{1}{2}} \tag{3.6}$$

For homogeneous isotropic turbulent flow the Smagorinsky constant, C_s is equal to 0.16 (Xu and Pope, 2000). In the Smagorinsky model the eddy viscosity co-efficient is maintained constant for the entire flow domain.

3.2.2 Particle Model

Aerosols were modeled as discrete particle tracks with the trajectories computed using the Lagrangian approach. The trajectory of the particle was determined by solving equation (3.7), where u_p is the velocity of the particle of mass m, at location x_i, F_G is the net gravitational force (Eq. 3.9), and F_D is the drag force (Eq. 3.10). C is the Cunningham correction factor, C_D is the drag coefficient, V_R is the relative velocity, d_P is the particle diameter, ρ_p is particle density, and ρ is the fluid density.

$$\sum F_i = m\frac{du_p}{dt} = F_D + F_G \tag{3.7}$$

$$\frac{dx_i}{dt} = u_p \tag{3.8}$$

$$F_G = \frac{1}{6}\pi d_p^3\Big(\rho_p - \rho\Big) \tag{3.9}$$

$$F_D = \frac{1}{8C}\pi d_p^2 \rho C_D |V_R| V_R \tag{3.10}$$

3.3 Numerical Scheme and Boundary Condition

The governing equations were discretized using the control volume method. A second order blended upwind scheme was applied for the convective-diffusive terms, and a forward Euler scheme was used for the temporal terms in the N-S equations. The boundary condition of the walls of the room represented no-slip conditions. Uniform velocity was specified at the inlets. The outlets were pressure boundaries with Dirichlet conditions applied for pressure and Neumann conditions for all other dependent variables.

Aerosols were initialized as described in Figure 2.4. The boundary conditions were set as per Table 2.3. The calculations for trajectories terminated when aerosols exited the room. When an aerosol struck a surface, it was assumed it bounced back with no energy loss representing an office with no 'soft' furniture such as carpets or sofas. The simulation assumed that the aerosols were spherical, had the properties of water and was neutral.

One-way coupling was applied i.e. it was assumed that the airborne particles had no influence on the surrounding air flow field and no particle-particle interaction occurred, which are valid given the low density of the aerosols released in the room scale. Resuspension was not considered. Inlet flow velocity was adjusted to obtain 3,

5, 7 ACH respectively. The particles were released randomly in a trapezoidal space within an area of 0.17 m^2 in a with a velocity range of 22-8 m/s.

3.4 Simulation Setup

The physical properties were set assuming the room temperature to be 27°C. Reynolds number was calculated for the inlet velocity adjusted to obtain three different ACH. It demonstrated that the turbulent flow was established in the space (Re $\approx$ 9,800, 16,000, and 24,000 for ACH 3, ACH 5, and ACH 7 respectively). For every simulation the air flow was first developed to ensure pseudo steady initial conditions were achieved and then the 'sneeze' happened. In each simulation, the size of the computational time domain was set to be a total of 9 minutes: 4 minutes for developing the air flow and then 5 minutes after releasing 150,000 particles.

The calculations were done in transient mode with .01 sec time step. In nearly all cases the particle diameter was maintained at 7 μm. For one case particles of multiple sizes (0.3, 1.0, 3.0, 7.0, 10 μm) were released. The Cunningham correction factor was included for particle sizes less than 5μm. the solver convergence was set to 0.0001 and minimum residual was specified as 10^{-5}. The particle release position, the furniture (in furnished room) and partition wall locations are identical for all cases. The inlet and outlet locations have been adopted as per the ventilation pattern.

3.5 Grid Sensitivity Analysis

In this study grid independence was assessed based on 15k, 25k, 50k, and 80k cells for one representative scenario (ACH=5, mixed cross ventilation, partition wall only). Figure 3.1 shows the vertical velocity profiles at different x locations (x = 1.17 m, 2.35 m, and 3.25 m), each using the four cell sizes mentioned before. The velocity profiles were obtained was studied after 4 minutes airflow. The velocity trend lines qualitatively show that increasing the grid resolution reduced the associated error.

(a)

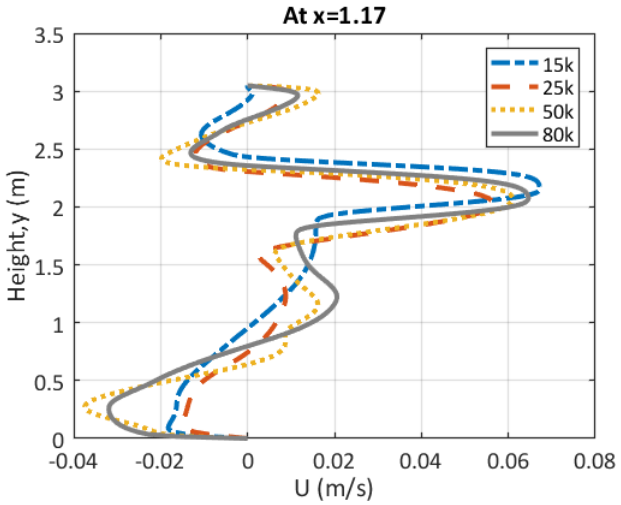

(b)

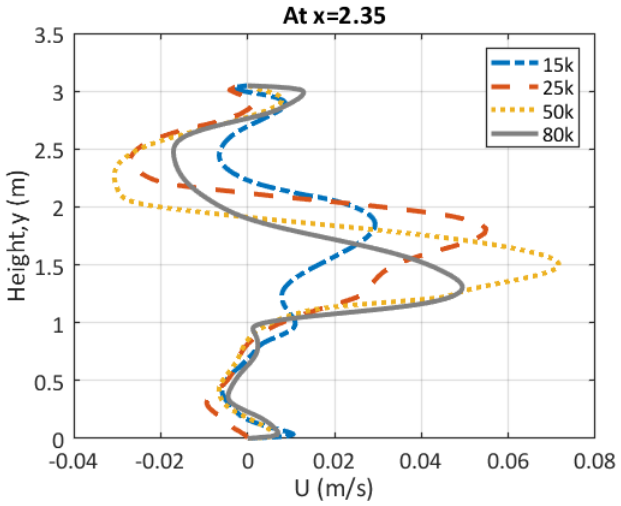

(c)

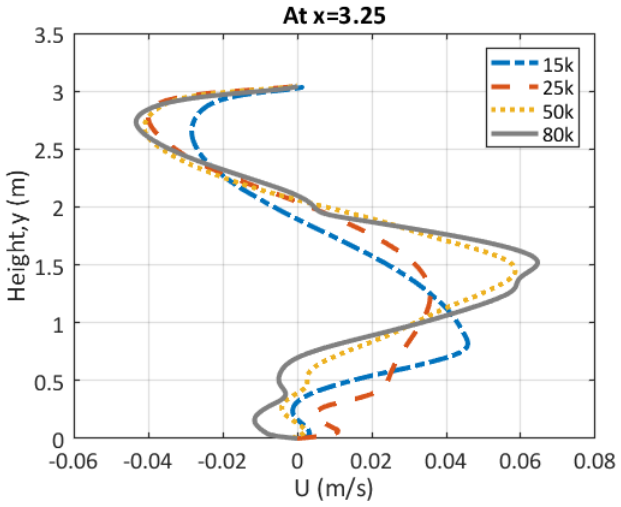

Figure 3.1 Vertical velocity profile at different locations: (a) at x=1.17 m, (b) at x=2.35 m, and (c) at x=3.25 m

With LES however, to obtain grid independence for a selected parameter, often the grid must be refined until it is nearly DNS and loses the fundamentals of LES. To ensure grid independence was achieved the grid convergence index (GCI) approach by Roache (1994, 1997) and Sørensen and Nielsen (2003) was applied.

Equation (3.11) was used to assess the uncertainty associated with grid resolution for predicting the solution f. Here f can be any given solution property of interest such as velocity magnitude in a point, number of particles in a space, or average temperature in the occupied zone. Roache (1997) recommends safety factor, $F_s = 3$ for normal applications. The formal order of accuracy p=2. The grid refinement ratio, r is calculated as $r = h_{coarse}/h_{fine}$, where h represents the cell size.

$$GCI_{fine,coarse} = F_s \left(\frac{f_{coarse} - f_{fine}}{1 - r^p} \right) \tag{3.11}$$

The GCI for two criteria outputs, velocity and particles remaining in the room i.e., $f = N/N_o$, and $f = U_{avg}$ was calculated. Since an output criteria in this study is the particle transport the solutions obtained for 80k, 50k, 25k, and 15k non-uniformed grids regarding particle number was compared. For this comparison h is taken as the maximum cell sizes. Figure 3.2 shows the comparative values of percentage of the particles in the breathing zone ($f = N/N_o$) for the cell number 15k, 25k, 50k and 80k. The GCI index was 8% when the grids were refined from 25k to 50k. It was <2% when the grids were refined from 50k to 80k indicating a grid resolution of 50k will result in an error margin of <2% compared to 80k.

Figure 3.3 represents the GCI analysis for the solutions of 80k and 50k grids where f is taken as the velocity of the airflow at three different point (x=1.17 m, x=2.35 m, x=3.2 5m). The GCI is not more than 2% at these positions and in the breathing zone the error is ≈1.5%. The GCI index from the velocity data shows that the grid resolution has minimal error margin with 50k grids.

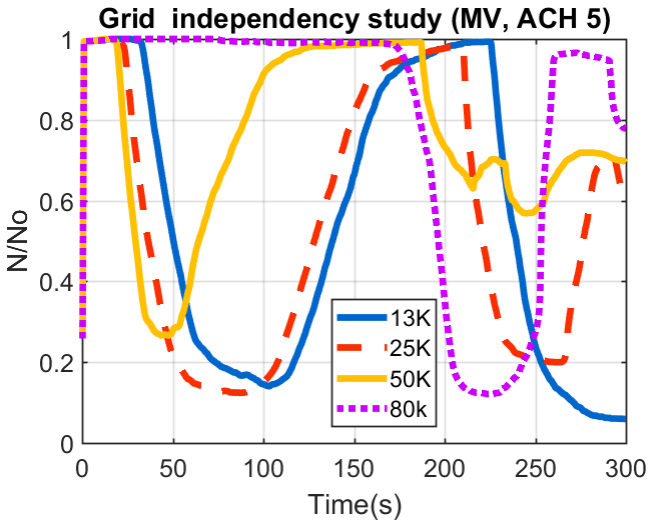

Figure 3.2 GCI index for particles remaining in the room: $GCI_{50,25} = 0.0845$, $GCI_{80,50} = 0.0217$

Computational time and data size are two important factors for CFD analysis. Table 3.1 shows how the time requirement for simulating the initial condition (IC), time requirement for particle simulation, and computer hard-disk memory space requirement increases with the increase of cell sizes. We can infer that increasing the cell number from 50k to 80k needs about 1.5 times more time and memory spaces with a minimal change in precision (GCI< 2%). With all these considerations, in the current study the grid resolution of 50k was chosen.

Table 3.1 Simulation study (LES)

Total cell number	**Time for IC simulation (hr)**	**Time for simulation with particles (hr)**	**Folder size (GB)**
15k	2	4	40
25k	4	5.5	41
50k	7.5	8	43
80k	11	12	62

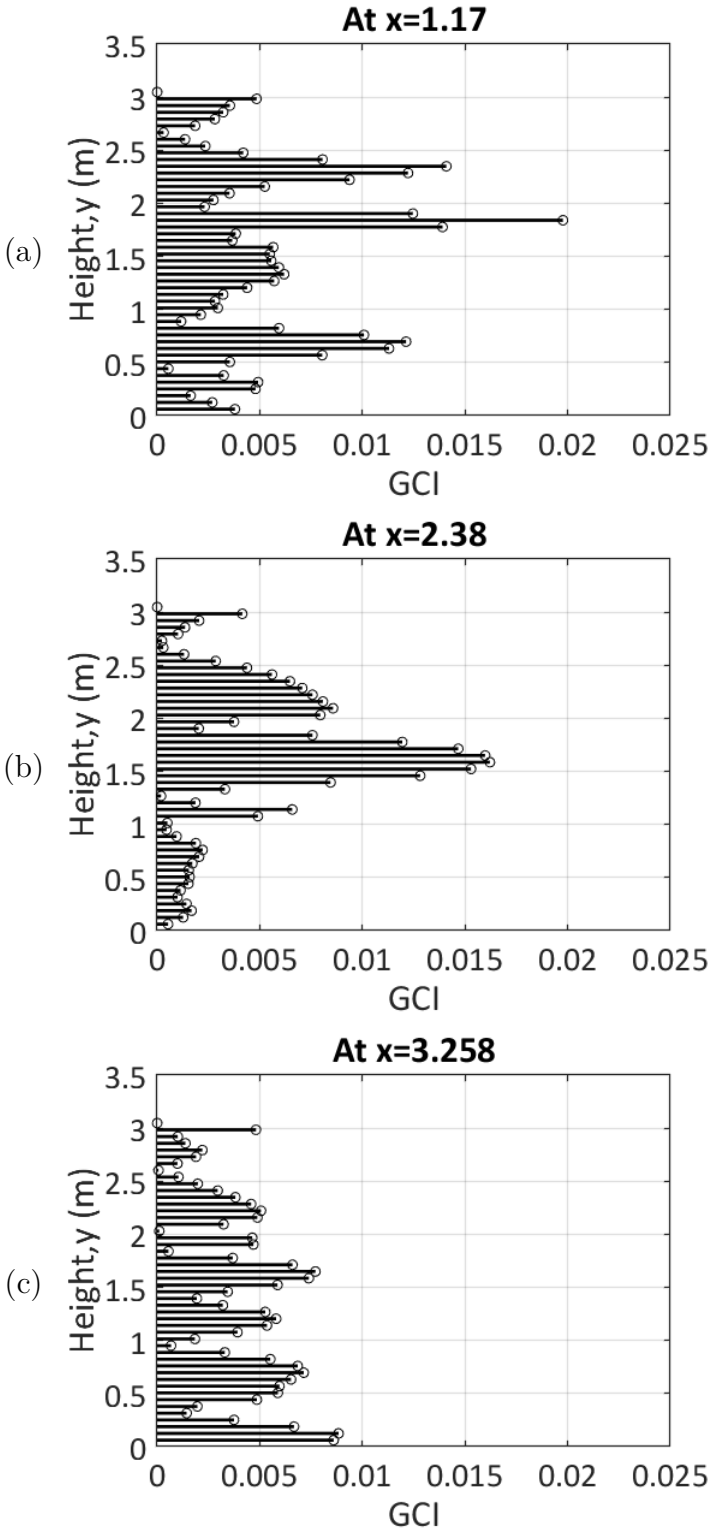

Figure 3.3 GCI analysis with velocity for 50K and 80K- (a) at x=1.17 m, (b) at x=2.35 m, and (c) at x=3.25 m

3.6 Model Validation

The governing physics of the developed CFD model for simulating air flow and particle transport has been applied and validated against experimental data (Hoque et al., 2009). This was performed by comparing the results from simulated environments found in literature against the experimental data for airflow and particle transport in an indoor ventilated space. The indoor air velocity measurement performed by Posner et al. (2003) and the particle mass concentration measurement performed by Lu et al. (1996) were used as benchmarks.

Chapter 4

Result and Discussion

This section presents the results of the 18 cases presented in Table 2.3. A pseudo steady initial condition was achieved developing air flow for 4 minutes. After that 150,000 particles each with a diameter of 7 μm were released and simulated for another 5 minutes. The air quality and the particle condition were observed after 9 minutes of simulation which was sufficient time for the particles to circulate the room.

To evaluate the air quality in the breathing zone and the whole domain, contour and bar plots were developed. Also, plots of velocity against height were generated to assess the variability in velocity in exhale and inhale zone. Particle number in the breathing zone and the room was analyzed along with the air quality to identify the best-case scenario for an efficient ventilation system. To understand the spatial and temporal particle pattern the number and location of particles in the breathing zone and the whole domain was also compared via statistical approaches We specified the zones as 'dead zone' where the magnitude of the air velocity is less than 0.005 m/s. The dead zone percentage and the particle number in the breathing zone as well as in the room varied as an impact of ventilation pattern, ACH and furniture layout.

4.1 Airflow

The velocity contour plots in Figure 4.1 show the resulting air flow pattern due to the different locations of the air flow inlet /outlet of the domain and in the presence/absence of desks for the same ACH of 5 at the end of nine minutes air flow.

(a) Case 2, $\mathbf{h_I/h_O = 1, D_{wo}/D_{wp} = 1}$ (b) Case 5, $\mathbf{h_I/h_O = 1, D_{wo}/D_{wp} < 1}$

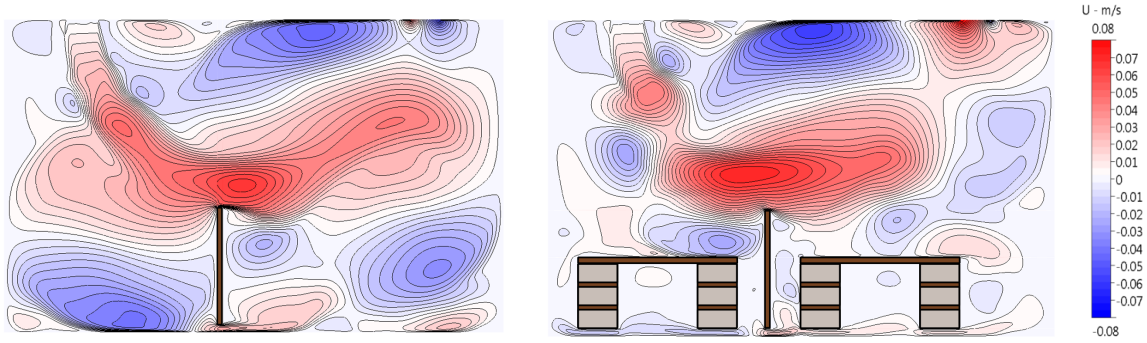

(c) Case 8, $\mathbf{h_I/h_O > 1, D_{wo}/D_{wp} = 1}$ (d) Case 11, $\mathbf{h_I/h_O > 1, D_{wo}/D_{wp} < 1}$

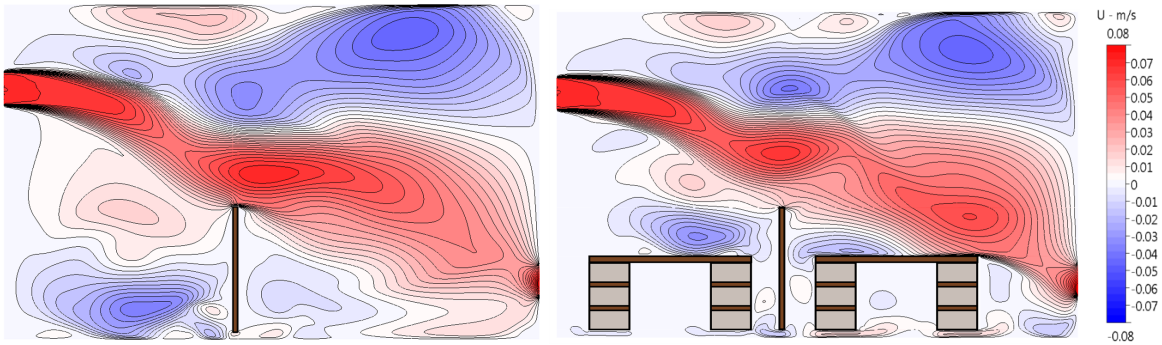

(e) Case 14, $\mathbf{h_I/h_O < 1, D_{wo}/D_{wp} = 1}$ (f) Case 17, $\mathbf{h_I/h_O < 1, D_{wo}/D_{wp} < 1}$

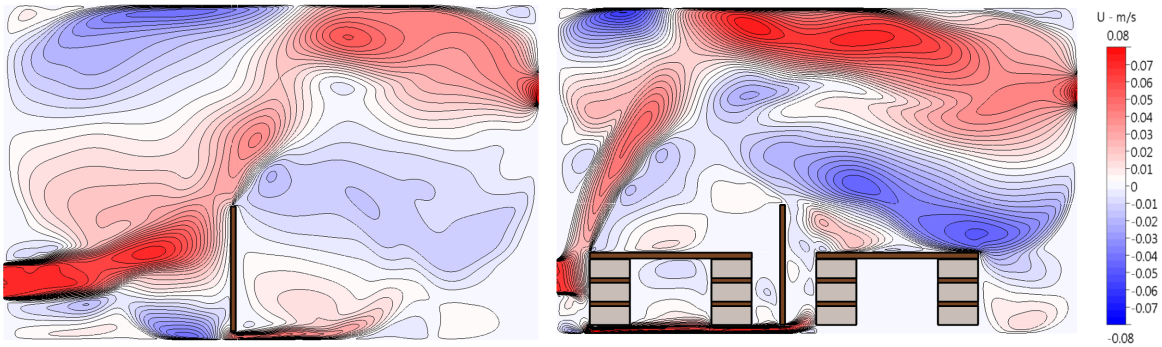

Figure 4.1 Velocity contour plots (ACH 5), (a) Case 2 (MV.Ceil), (b) Case 5 (MV.Ceil), (c) Case 8 (MV.Cross), (d) Case 11 (MV.Cross) , (e) Case 14 (DV.Cross) , and (f) Case 17 (DV.Cross).

Regions in the room hovering near white depict areas with velocities oscillating around zero. High positive velocities are concentrated in the pathways from the inlet to the outlet and immediate recirculation zones are created around it. From the observation of case 2 (MV.Ceil, $D_{wo}/D_{wp} = 1$), and case 5 (MV.Ceil, $D_{wo}/D_{wp} <$

1), where both inlet and outlet are located in the ceiling, we can notice that in case 2,Figure 4.1(a), the circulations with higher velocities are in the upper regions of the room and at the corners. For case 5, Figure 4.1(b), the presence of desks results in near zero velocity magnitudes. This is noted in other cases as well, the velocities oscillate near zero at the region near or below the desk.

In Figures 4.1(c) and (e) where the inlet/outlet locations are reversed the flow pattern appears 'inverse' with higher velocity magnitudes at the inhalation zone for Case 8 ($h_I/h_O > 1$, $D_{wo}/D_{wp} = 1$) and Case 14 ($h_I/h_O < 1$, $D_{wo}/D_{wp} = 1$). Case 11 ($h_I/h_O > 1$, $D_{wo}/D_{wp} < 1$), Figures 4.1 (d), appears similar to Case 8 (Figures 4.1(c)), even though desks are present. The relative location of the inlet/outlet to the position of the desks result in lesser impact on the air flow pattern when the inlet is above the outlet or both are located at the top. This is obvious when comparing cases 14 (Figures 4.1(e)) and 17 (Figures 4.1(f)). In case 17 ($h_I/h_O > 1$, $D_{wo}/D_{wp} < 1$), the desk is located in front of the inlet. This causes the air flow trajectory to move upwards, very different from case 14.

Changing the ACH immediately influenced the extent of white in the plots as shown in Figures 4.2 and 4.3. Figure 4.2 and Figure 4.3 shows the velocity contour plots in the presence and absence of the of desks respectively for ACH = 3 and 7 for MV.Ceil ($h_I/h_O = 1$), MV.Cross ($h_I/h_O > 1$) and DV.Cross ($h_I/h_O < 1$). At both ACH the flow pattern remains unchanged and at ACH = 7, we appear to have less zones with very low velocities, but the locations remain nearly the same, the corners, around the partition and below the desks (Figure 4.2).

The only deviation is case 18 (ACH 7, DV.Cross, $D_{wo}/D_{wp} < 1$),(Figure 4.2 (f)), where the upper corners have higher velocities because of the relative placement of the desks. Figure 4.3, which shows results for lower ACH, mixed cross ventilation creates a dead chunk in the exhale area and in displacement ventilation the dead chunk is created in the inhale portion. The partition wall has an impact on this fact.

These dead chunks are reduced when high ACH is offered.

So, from the visual expression of the contour plots it can be inferred that in lower ACH, mixed ceiling ventilation ($h_I/h_O = 1$), gives better air flow where there are partition walls and no desk in the domain ($D_{wo}/D_{wp} = 1$). From the contour plots, we observe that increasing ACH makes the air flow more sensitive with the presence of furniture with respect to mixing in the domain and the number of zones with velocity extremes.

(a) Case 4, **ACH=3**, $\mathbf{h_I/h_O = 1}$ (d) Case 6, **ACH=7**, $\mathbf{h_I/h_O = 1}$

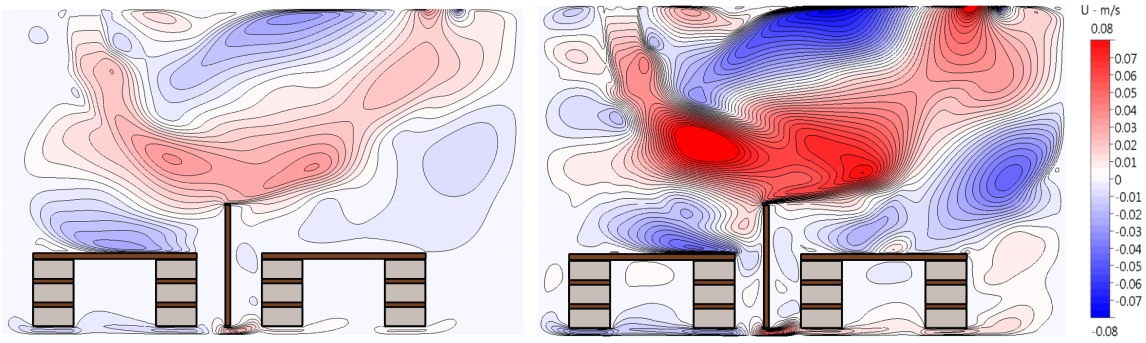

(b) Case 10, **ACH=3**, $\mathbf{h_I/h_O > 1}$ (e) Case 12, **ACH=7**, $\mathbf{h_I/h_O > 1}$

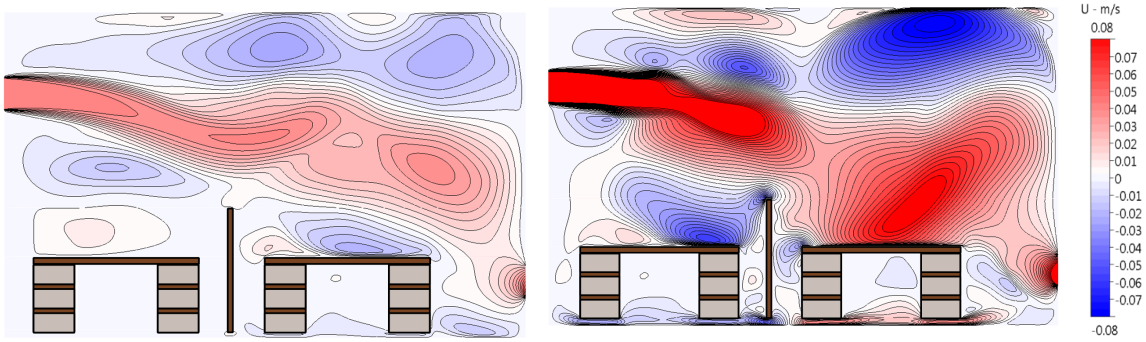

(c) Case 16, **ACH=3**, $\mathbf{h_I/h_O < 1}$ (f) Case 18, **ACH=7**, $\mathbf{h_I/h_O < 1}$

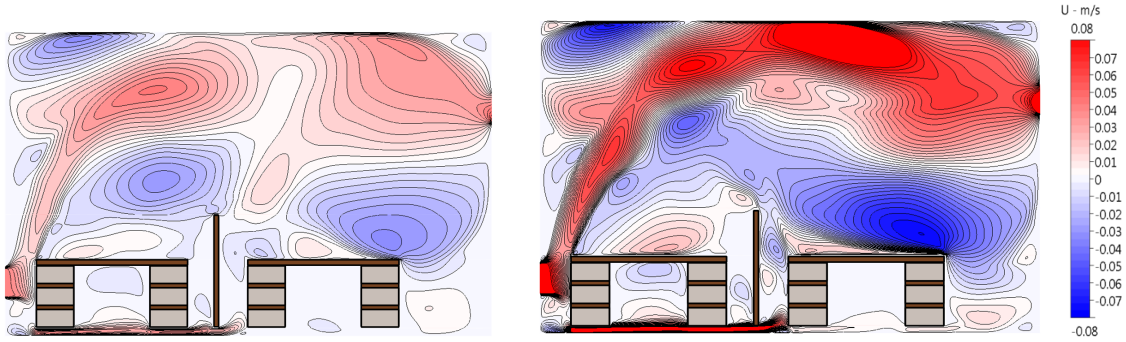

Figure 4.2 Velocity contour plots, (a) Case 4, (b) Case 10, (c) Case 16, (d) Case 6, (e) Case 12, and (f) Case 18.

Doing a qualitative check through comparison of the contour plots gives a visual interpretation of the impact of changing the three variables. From the height vs. normalized average velocity (U_{avg}/U_o , where U_o is the inlet velocity), velocity plot in inhale and exhale area (Figure 4.4 and Figure 4.5), we can find similar scenario-

higher ACH creates more flow in the breathing zone, significantly in the inhale area than the lower ACH. Assessing through the multiple configurations for velocity line plits accross the room heoght atspecific locations is revealing. Velocity profile was analyzed at two x locations, $x = 1.06$ m (exhale zone) and 3.19 m (inhale zone). The locations were chosen such that edge effects from the desks or the walls was minimized.

Analyzing the impact of increasing ACH on the velocity profile, we observed that for displacement ventilation increasing the ACH from 5 to 7 does not make significant changes in velocity conditions for both room conditions (with and without the desks). Figure 4.6 shows the normalized average velocity line plots for the cases having displacement ventilation (H_I/H_o <1). Figure 4.6 (a,b) is a plot of the Normalized average U velocity lines where $D_{wo}/D_{wp} = 1$, for cases 13 (ACH 3), 14 (ACH 5), 15 (ACH 7) and Figure 4.6 (c,d) is a plot of the Normalized average U velocity lines where $D_{wo}/D_{wp} < 1$, for cases 16 (ACH 3), 17 (ACH 5), 18 (ACH 7). In the exhale region, Figure 4.6 (a), the lines for cases 14 and 15 nearly overlap. In the exhale region, Figure 4.6 (a), for cases 14 and 15 the pattern is the same with the magnitude higher for case 15,where ACH = 7. Case 13 with ACH = 3 is different from case 14 (ACH 5) significantly in inhale zone while the line plots look similar for case 14 and 15 (Figure 4.6 (b)). In the cases with the desks, Figure 4.6 (c) shows the Normalized average U velocity lines in exhale zone for cases 16, 17, 18 overlap each other. In the inhale region, Figure 4.6 (d), case 17 and case 18 appears almost similar.

Assessing the significance of ventilation pattern, we can infer that, at ACH = 3 changing the ventilation pattern had a significant impact in the presence and absence of desks but not at ACH of 5 and 7. This indicates at lower ACH, the room characteristics and air flow rate take on greater importance on the air flow pattern. At ACH = 5 and 7 the significance is less.

For the cases 5 ($h_I/h_O = 1$), 11 ($h_I/h_O > 1$), 17 ($h_I/h_O < 1$) and cases 6

(a) Case 1, **ACH=3**, $\mathbf{h_I/h_O = 1}$ (d) Case 3, **ACH=7**, $\mathbf{h_I/h_O = 1}$

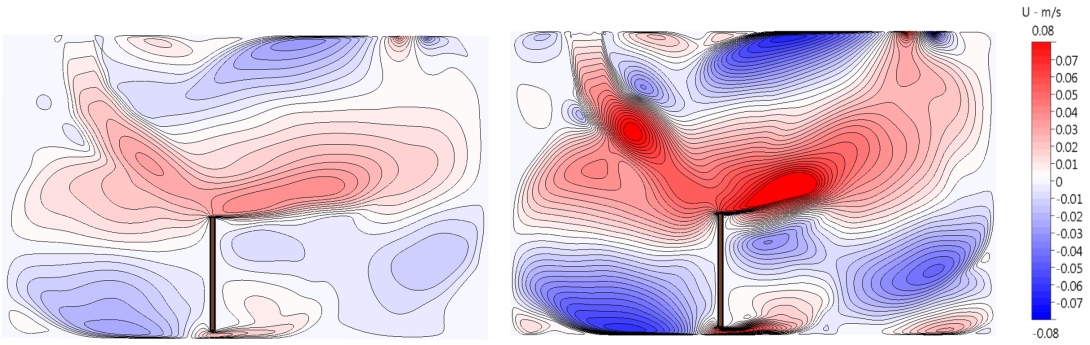

(b) Case 7, **ACH=3**, $\mathbf{h_I/h_O > 1}$ (e) Case 9, **ACH=7**, $\mathbf{h_I/h_O > 1}$

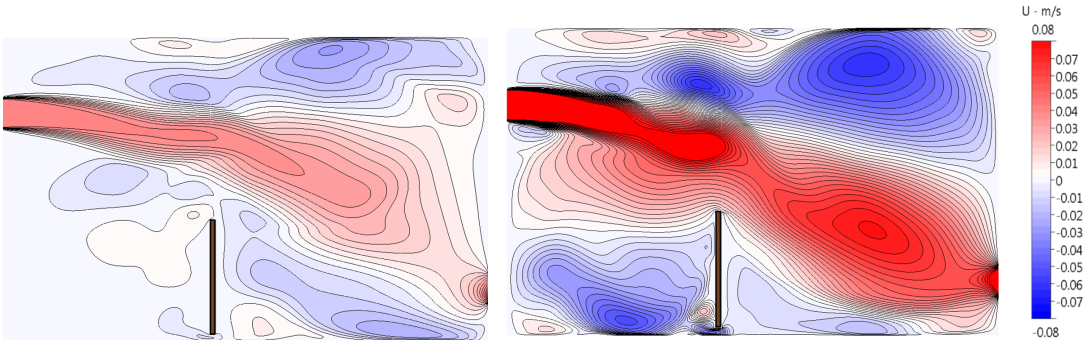

(c) Case 13, **ACH=3**, $\mathbf{h_I/h_O < 1}$ (f) Case 15, **ACH=7**, $\mathbf{h_I/h_O < 1}$

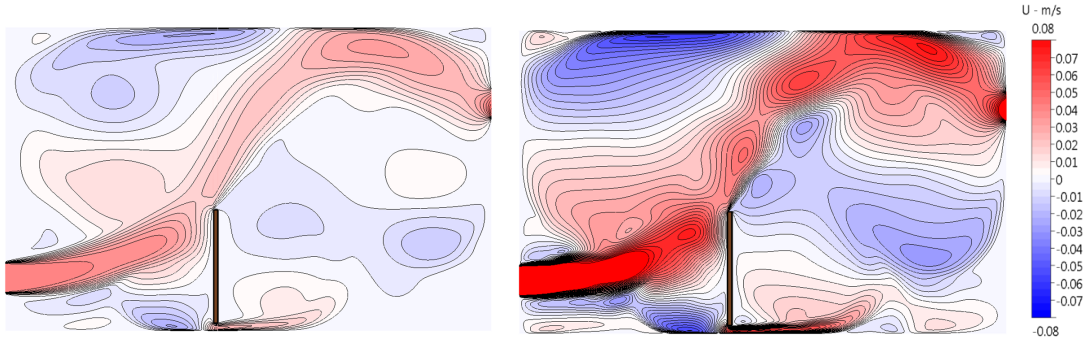

Figure 4.3 Velocity contour plots, (a) Case 1, (b) Case 7, (c) Case 13, (d) Case 3, (e) Case 9, and (f) Case 15.

($h_I/h_O = 1$), 12 ($h_I/h_O > 1$), 18 ($h_I/h_O < 1$), where the domain had partition wall and desk and having ACH 5 and ACH 7 respectively, the impact on the ventilation pattern was insignificant both in inhale and exhale area (Figures 4.7(c, d) and Figures 4.8 (c, d)).

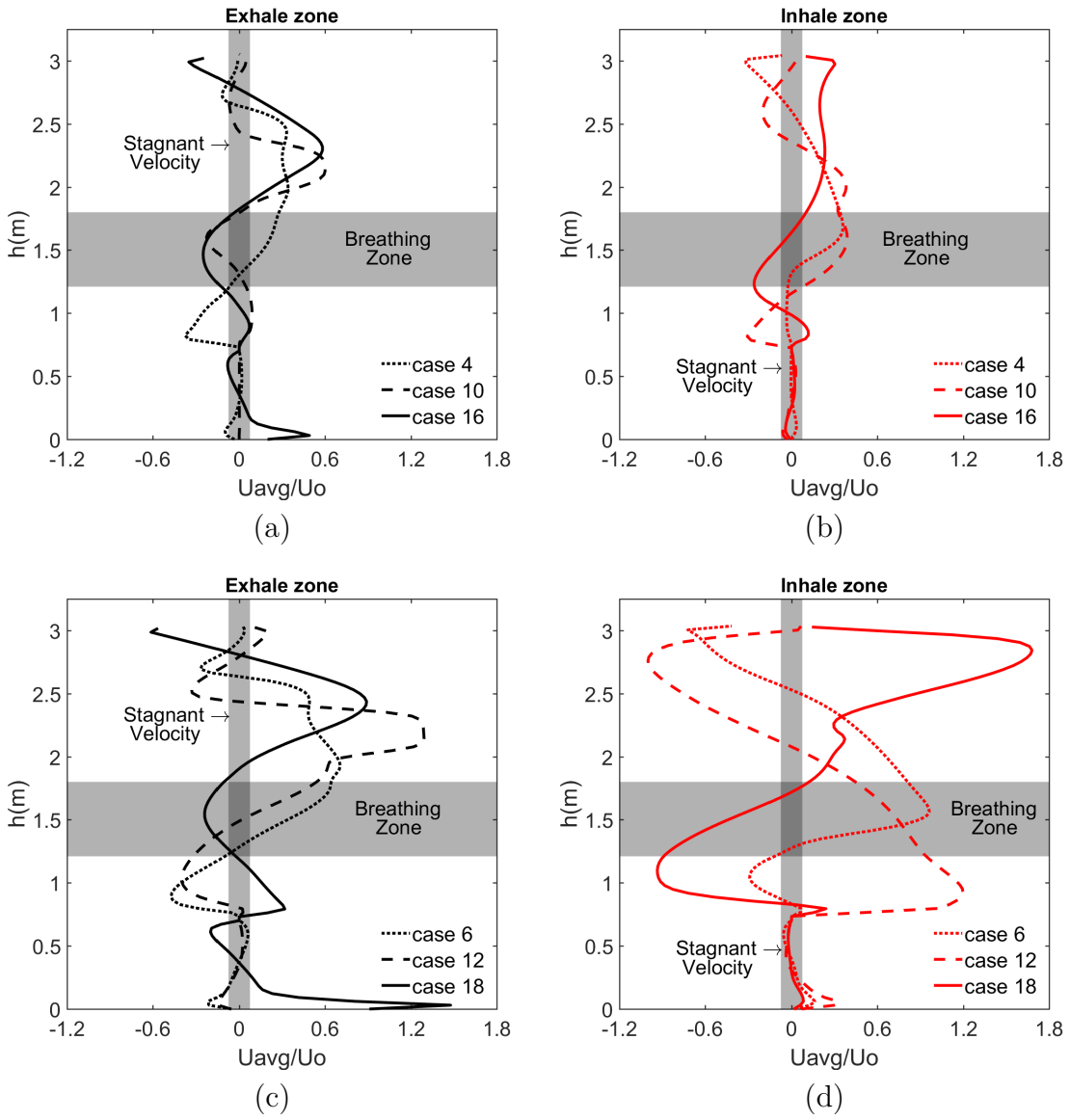

Figure 4.4 Normalized average velocity line plots (cases where $D_{wo}/D_{wp} < 1$), (a) exhale zone and (b) inhale zone for case 4 (ACH 3, $h_I/h_O = 1$), case 10 (ACH 3, $h_I/h_O > 1$), and case 16 (ACH 3, $h_I/h_O < 1$) and (c) exhale zone and (d) inhale zone for case 6 (ACH 7, $h_I/h_O = 1$), case 12 (ACH 7, $h_I/h_O = 1$), and case 18 (ACH 7, $h_I/h_O < 1$).

In some cases the velocity profile change was significant in the exhale zone but not in the inhale zone. For example, in cases 1 (ACH 3, $h_I/h_O = 1$, $D_{wo}/D_{wp} = 1$), 7 (ACH 3, $h_I/h_O > 1$, $D_{wo}/D_{wp} = 1$)and 13 (ACH 3, $h_I/h_O < 1$, $D_{wo}/D_{wp} = 1$) going from case 1 to 13, the change has an impact in both exhale and inhale zones

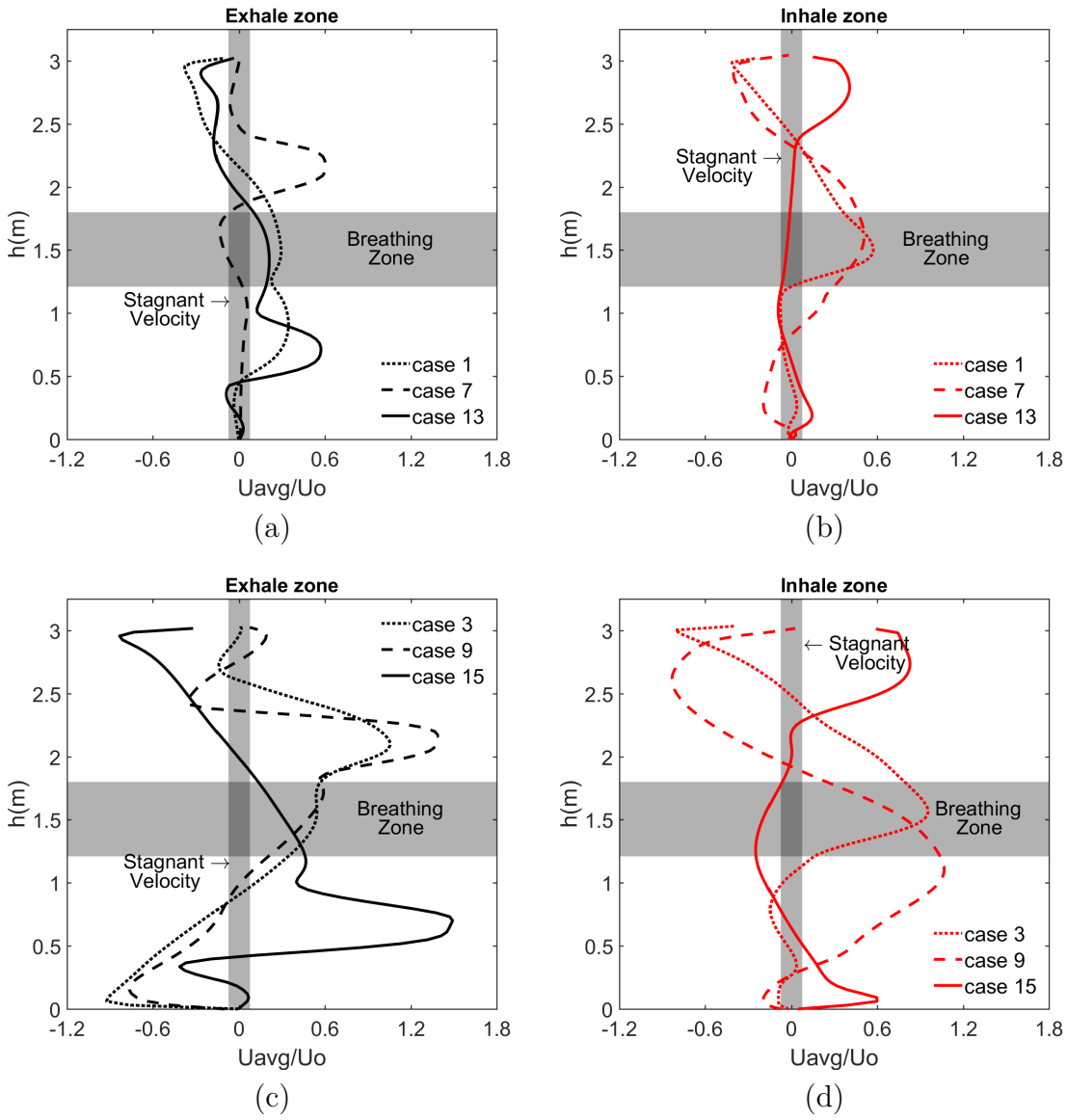

Figure 4.5 Normalized average velocity line plots (cases where $D_{wo}/D_{wp} = 1$), (a) exhale zone and (b) inhale zone for case 1 (ACH 3, $h_I/h_O = 1$), case 7 (ACH 3, $h_I/h_O > 1$), and case 13 (ACH 3, $h_I/h_O < 1$) and (c) exhale zone and (d) inhale zone for case 3 (ACH 7, $h_I/h_O = 1$), case 9 (ACH 7, $h_I/h_O > 1$), and case 15 (ACH 7, $h_I/h_O < 1$).

(Figures 4.5 (a, b)), i.e. when the inlet and outlet locations moved from the ceiling to the opposite ends of the wall.

In cases 3 (ACH 7, $h_I/h_O = 1$, $D_{wo}/D_{wp} = 1$), 9 (ACH 7, $h_I/h_O > 1$, $D_{wo}/D_{wp} = 1$)and 15 (ACH 7, $h_I/h_O < 1$, $D_{wo}/D_{wp} = 1$) going from 3 and 9 , the impact

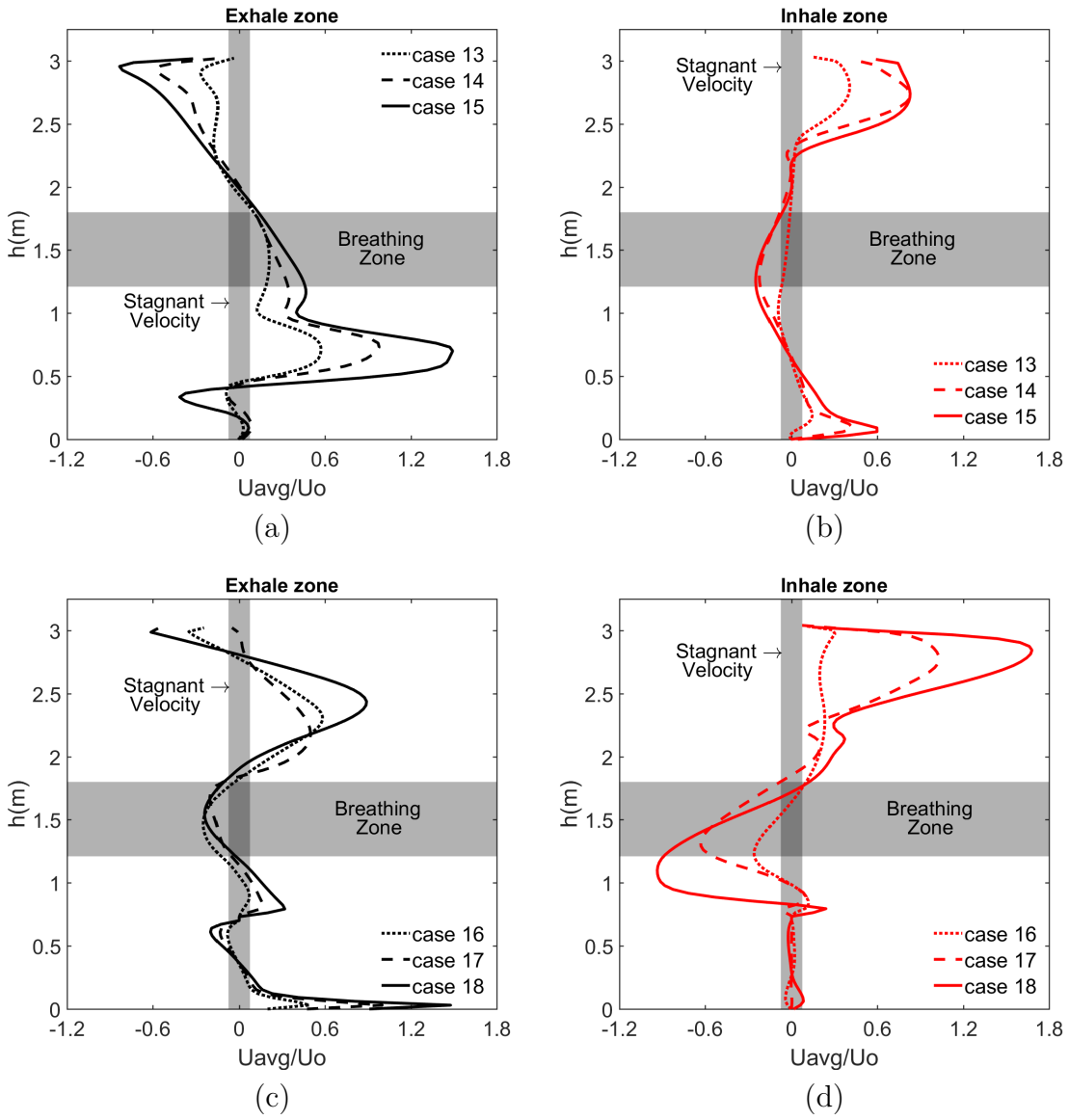

Figure 4.6 Normalized average velocity line plots, (a) exhale zone and (b) inhale zone for cases 13, 14, and 15 and (c) exhale zone and (d) inhale zone for cases 16, 17, and 18.

was significant in the inhale zone (Figure 4.5(d)) but not in the exhale zone (Figure 4.5(c)). This could be because before crossing the partition the effects of the location persisted but smeared out after the partition. However, it is interesting to note that when desks were absent the ventilation pattern had more significant scenarios than in the presence of desks. This could be because there was more void space for the

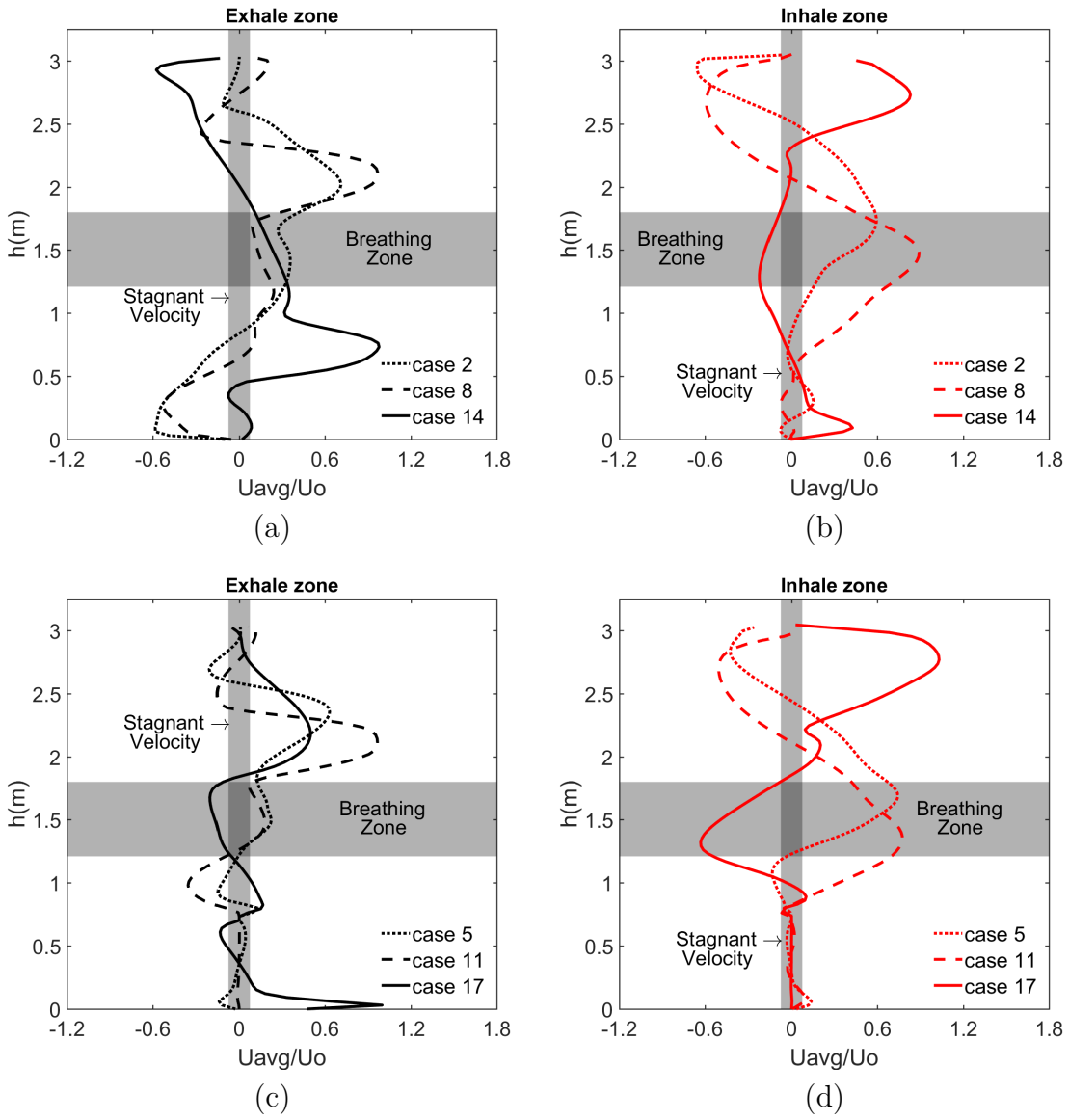

Figure 4.7 Normalized average velocity line plots, (a) exhale zone and (b) inhale zone for cases 2, 8, and 14 and (c) exhale zone and (d) inhale zone for cases 5, 11, and 17.

flow to take shape.

At higher air changes the interior arrangement in mixed ventilation, where as in displacement ventilation the presence of desk play role in the air flow pattern. This is because in the displacement ventilation the desk changes the direction of the flow in the first place. In Figure 4.9, the normalized velocity line plots in exhale and

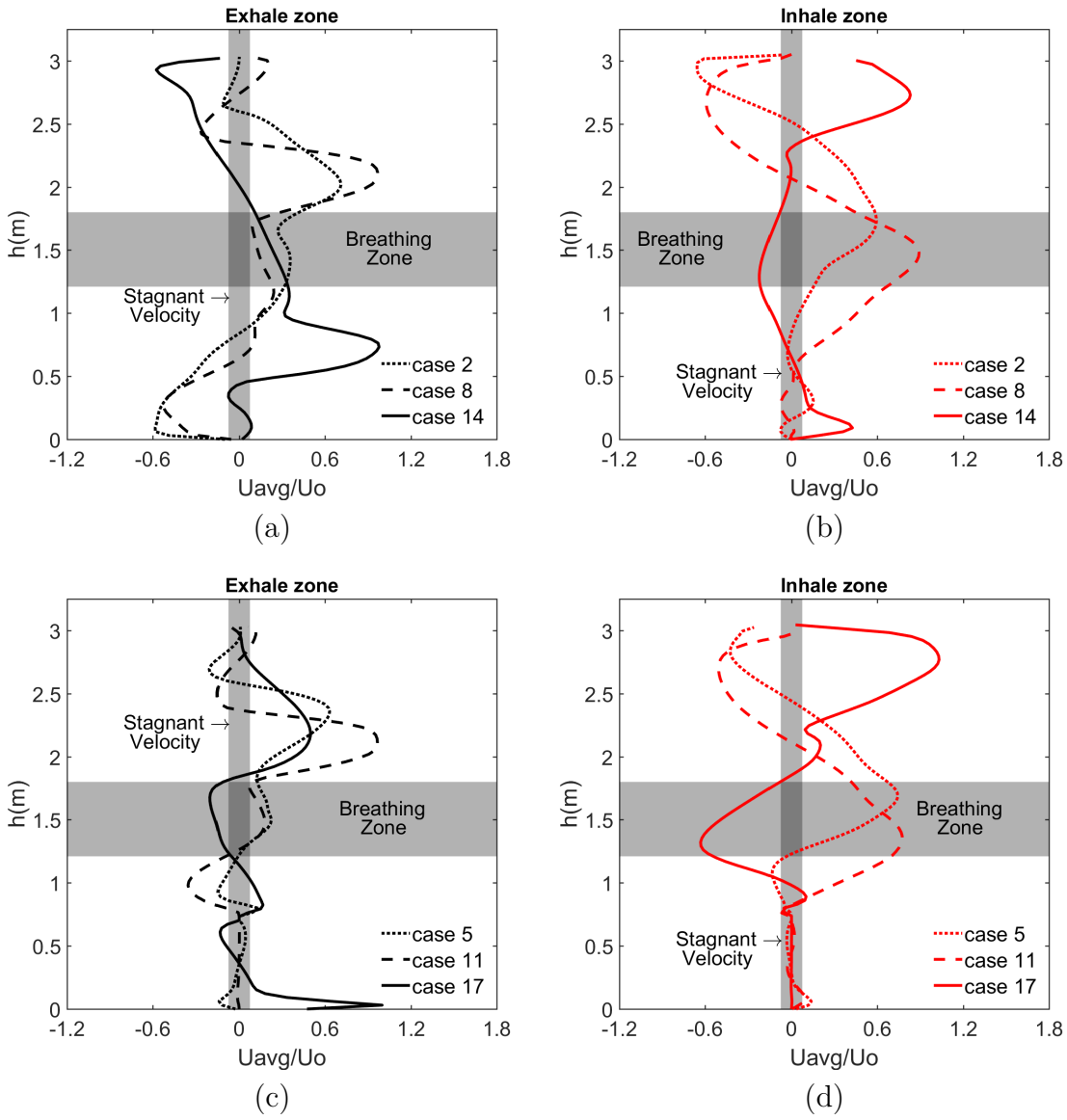

Figure 4.8 Normalized average velocity line plots, (a) exhale zone and (b) inhale zone for cases 4, 10, and 16 and (c) exhale zone and (d) inhale zone for cases 6, 12, and 18.

inlet zone for case 3 (ACH 7, $h_I/h_O = 1$, $D_{wo}/D_{wp} = 1$),case 6 (ACH 7, $h_I/h_O = 1$, $D_{wo}/D_{wp} < 1$) and case 9 (ACH 7, $h_I/h_O > 1$, $D_{wo}/D_{wp} = 1$), case 12 (ACH 7, $h_I/h_O > 1$, $D_{wo}/D_{wp} < 1$) is presented. Here, it is observed that, the velocity line plots are similar up to the breathing zone and near the floor area the velocity falls in the stagnant area where the desks are introduced. So, in displacement ventilation

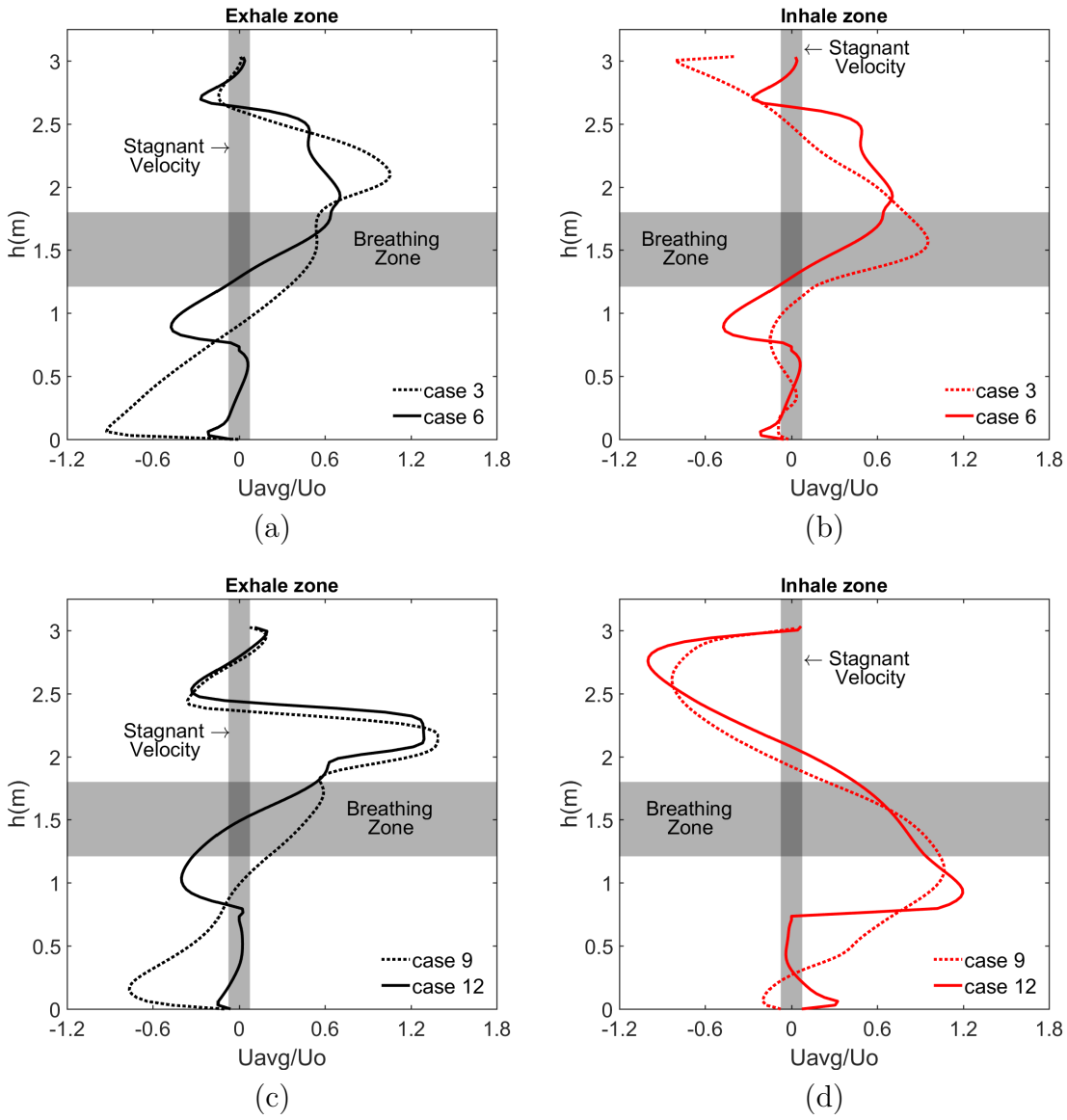

Figure 4.9 Normalized average velocity line plots, (a) exhale zone and (b) inhale zone for cases 3, 6 (c) exhale zone and (d) inhale zone for cases 9, 12.

(where, $h_I/h_O < 1$), the impact is exposed more significantly. In displacement ventilation, at ACH 3 this impact is not significant in exhale area, where for higher ACH the presence of desks is significantly impact the flow in both inhale and exhale area. For ACH of 3 and 5, r

elative location of the inlet, outlet and the position of the desks as well as their presence or absence influences the velocity pattern.

To analyze the air circulation quality in the domain, we have identified the proportions of the areas having stagnant velocity (Uavg $<|0.005\ ms^{-1}|$). Figures 4.10, 4.11, and 4.12 shows the percentage of dead zone (possesses stagnant velocity) and well air-circulated zones after 9-minute air flow in the total domain at ACH 3, ACH 5 and ACH 7 respectively. We have assumed the breathing zone from 1.21 m to 1.80 m from the floor level, that possesses 19% of the total domain. At ACH 3 (Figure 4.10), the ventilation pattern is not significant for the total air flow condition (non-stagnant area 50% for all ventilation pattern) but in the breathing zone the ceiling ventilation offers more air circulation (non-stagnant area in the breathing zone is 80%) than both types of cross ventilations (non-stagnant area in the breathing zone is 50%). This fact can be explained from the velocity contour plots in Figure 4.3. the partition wall has an impact on the air flow in the breathing area. For the cross ventilations (Figure 4.3 (b) and Figure 4.3 (c)), a larger dead zone portion is created at one side of the partition wall (in exhale area for MV and in inhale area for DV) than the ceiling ventilation (Figure 4.3 (a)).

If we look into the effect of furniture on the dead zone percentage in the breathing zone and non-breathing zone, in the mixed ceiling ventilation, the air flow dominates the upper portion of the room, so the dead air pockets created around the furniture keep increasing over time. So, the dead zone in the total room appears more than other ventilation patterns. On the other hand, presence of furniture lessens the dead zone in total in the displacement ventilation. The effect of furniture on the dead zone percentage is minimal in the mixed cross ventilation.

Tables 4.1 and Table 4.2 summarize the result of dead zone percentage in a room with a partition wall and a room with partition wall and desk respectively. In both room conditions, increasing ACH lessens the dead zone in breathing as well as non-

Table 4.1 Percentage (appx.) of dead zone in the room with partition wall only.

ACH	MV Ceil.		MV Cross		DV Cross	
	N. Br. Z.	Br. Z.	N. Br. Z.	Br. Z.	N. Br. Z.	Br. Z.
3	41	4	42	10	42	10
5	28	3	24	3.5	28	3
7	22	3	15	4	20	4

Table 4.2 Percentage (appx.) of dead zone in the room with partition wall and desks.

ACH	MV Ceil.		MV Cross		DV Cross	
	N. Br. Z.	Br. Z.	N. Br. Z.	Br. Z.	N. Br. Z.	Br. Z.
3	45	6.5	37	7	31	5
5	36	3	29	3.5	26	3
7	27	4	23	2	19	2.5

breathing zones. Increase the ACH from 3 to 7 in a room with only partition wall decrease the dead zone 50-65% for all type of ventilation, and in ta room with partition wall and desk, the decrease is 40. Dead zone in the breathing area are less sensitive with the ventilation pattern with ACH 5 and ACH 7. In the room with a partition wall and desks, displacement ventilation offers least dead zone and mixed ceiling ventilation creates maximum dead one regardless the ventilation pattern (Table 4.2).

4.2 Particle Transport

Particle transport and air flow quality in a space are directly inter-related. A well-ventilated room offers faster removal of the infectious particles from the room. We can observe both the air flow condition and the particle quantities from Figures 4.10,

4.11, and 4.12. This information along with the total particles stayed in the room, the pattern of their trajectory as well as their location (inhale or exhale zone) are required to reach a conclusion about particle transport behavior.

For example, if we look at Figure 4.10, we find that with ACH 3 the particles do not leave the domain in 5 minutes, regardless of the ventilation pattern or the room condition. However, in the breathing zone displacement ventilation (case 13 and case 16) offers least number of particles after 5 minutes of the release. For case 13 (ACH 3, $h_I/h_O<1$, $D_{wo}/D_{wp}=1$), we see that only 1.3% particles remain in the breathing zone.

In Figure 4.13(a), we can observe that after ≈3.5 min the number of the particles starts to fall off. However, from Figure 4.17, where the location of the particles over time can be analyzed, we find that for case 13 the particles stay mostly in the exhale zone. They do not pass the partition wall (Figures 4.17 a,b).

From the change of y-coordinates we observed that they gradually exit from the breathing zone and at ≈3.5 min the move out from the breathing zone (Figures 4.17 c, d). Similar scenario is observed for case 16 (ACH 3, $h_I/h_O<1$, $D_{wo}/D_{wp}>1$).

Although the least number of the particles (≈3%) is in the breathing zone, the particles recirculated to the zone. From Figure 4.14(a) we can see the particle numbers peak at ≈100 sec and ≈200 sec. Here, the particles dispersed horizontally (Figures 4.17 a, b) due to the velocity vortex near the desk (Figure 4.2c). The particles mostly stayed in the breathing level except from ≈90-180 sec and they started to leave the breathing level at ≈3.5 min and cluster near the ceiling (Figure 4.17 c, d).

These facts can be explained from the velocity contour plot at Figure 4.3(c) and Figure 4.2(c). For the displacement ventilation with ACH 3, the inhale area built up a negative and stagnant velocity portion. So, it can be inferred that although the quantity of the particles is showing less in the breathing zone after 5 minutes, the chance of removal the infectious particles from the room is negligible. The par-

ticles mostly remained in the near the exhale area and they might come back to the breathing zone after a while.

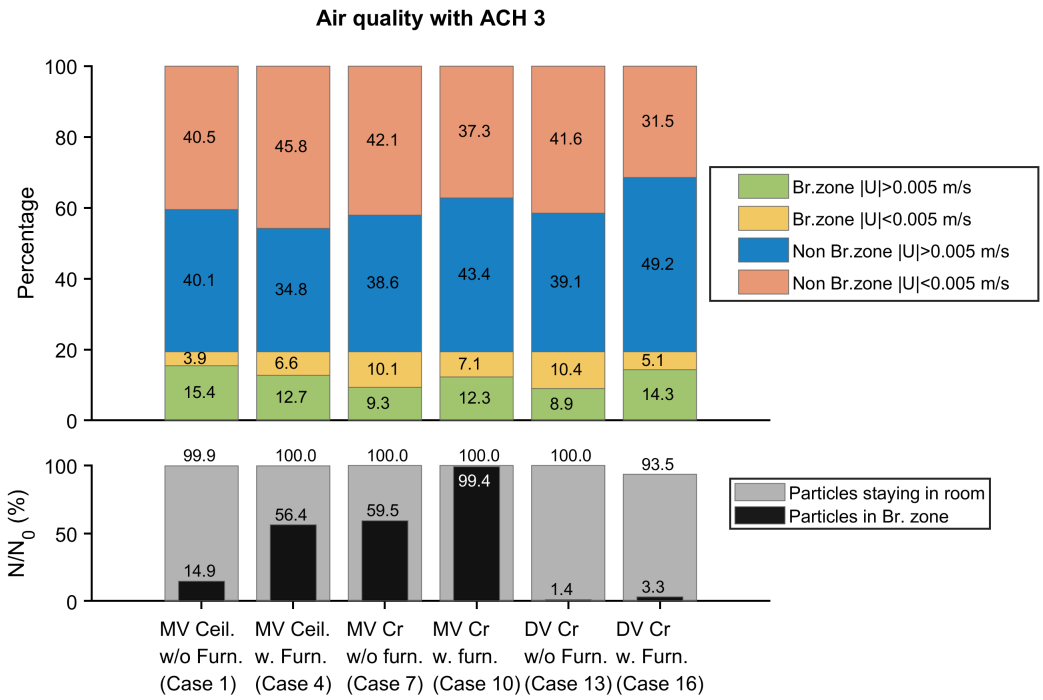

Figure 4.10 Effect of ventilation pattern on air quality and particle concentration in the breathing zone at ACH 3.

Increasing ventilation rate to ACH 5 has more impact on ceiling (h_I/h_O=1) and displacement (h_I/h_O<1) ventilation than mixed cross ventilation (h_I/h_O>1) in removal of particles from the domain and from the breathing zone (Figure 4.11). For the case where (D_{wo}/D_{wp}<1), ceiling ventilation (h_I/h_O=1) has ≈80% less particles in the breathing zone than the displacement (h_I/h_O<1) ventilation having ≈12% less particles in the total domain. Particle concentration in the breathing zone over time for cases 2, 14 and cases 5, 17 is analyzed from Figure 4.13(b) and 4.2(b) respectively. The cases where D_{wo}/D_{wp}=1, the number of the particles started to increase at ≈100 s, reached at its peak at ≈200 s, and then dropped to ≈19% after 5 min. From Figures 4.15(a, b), we observe that the particles were on average in the exhale

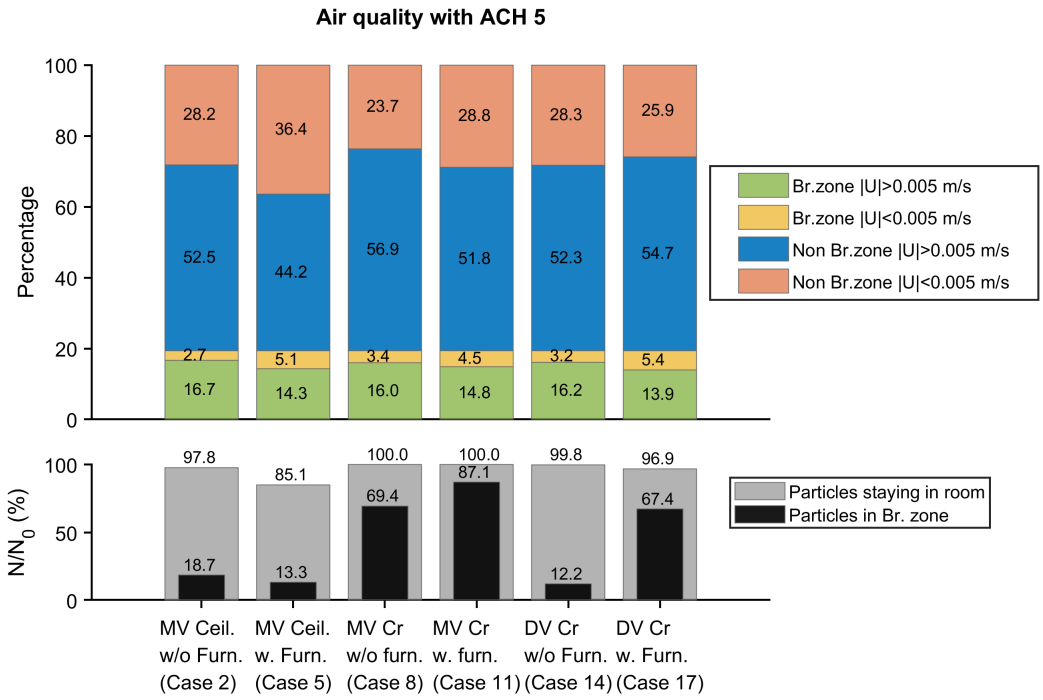

Figure 4.11 Effect of ventilation pattern on air quality and particle concentration in the breathing zone at ACH 5.

area and started to spread after 1 min (except the 3rd min.). Except from ≈100s to ≈150s, the particles mostly remained below the breathing zone and at ≈ 210s, the particles started to enter the breathing zone from below (Figures 4.15 (a, b)). So, it can be inferred that around 4 min the particles would transport to the breathing zone and as they were more dispersed by that time, the concentration at the peak could be small and removal from the domain could not be confirmed.

For displacement ventilation (h_I/h_O<1) where D_{wo}/D_{wp}=1, the scenario was quite similar with the case having ACH 3 (Case 13). As the air flow pattern remained unchanged having less dead zones and higher velocity vortexes (Figure 4.1(e), the particles trapped in the exhale area oscillated faster. The particles started to move out from the breathing zone earlier (≈30s) but the oscillating motion brought them back at ≈230s (Figure 4.15(e), 4.17(c, d)). So, although it seemed that the number of the

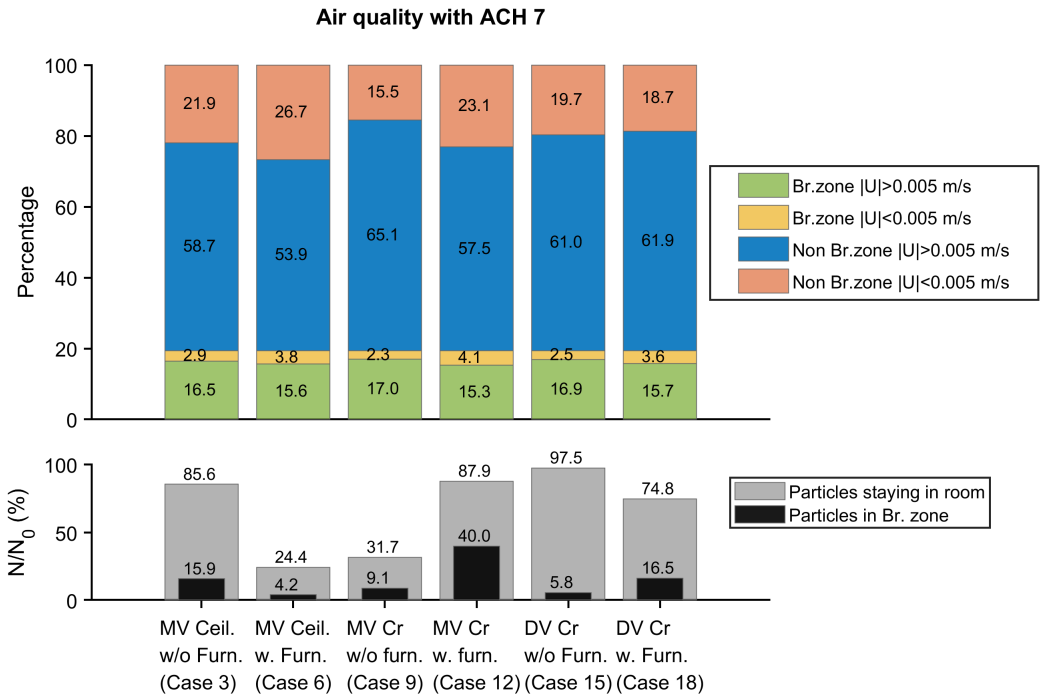

Figure 4.12 Effect of ventilation pattern on air quality and particle concentration in the breathing zone at ACH 7.

particles in the breathing zone in a room with a partition wall (D_{wo}/D_{wp}=1), having ventilation rate of ACH 5, the displacement ventilation (h_I/h_O<1) offered less number than ceiling ventilation (h_I/h_O=1), in displacement ventilation the particles trapped in the upper portion exhale zone and have tendency to circulate there resulting higher frequency of return with almost same concentration as they did not disperse much and decline to move to the exit zone.

With the presence of desks (D_{wo}/D_{wp}<1), the air circulation pattern and the particle transport were more complex. From Figure 4.14(b), we can observe that in the ceiling ventilation, the particle number reaches at its peak at ≈90s then gradually dropped ≈13% at 5 minutes. The particles started scattering after ≈2 min both horizontally and vertically (Figure 4.15 (a, b) and (c, d)). Although case 5 showed more dead-zone than case 17 (displacement ventilation, h_I/h_O<1), from Figure 4.1

(b), we can observe that in ceiling ventilation (case 5), the dead zones are located near the boundary walls and below the desks and both sides of the partition wall have better air circulation that helps the transport the particles to move out from the breathing zone as well as to the exit portion.

Although displacement ventilation (case 17) ends up with 30% less dead zone that ceiling ventilation (case 5), Figure 4.1 (f) shows it creates a dead zone portion at the exhale zone near the partition wall, that can trap some particles. From Figure 4.17(a, b), it is noticed that after ≈100 s the particles moved to the inhale zone and also removed from the breathing zone 4.17(a, b), but the flow pattern shows that the particles tends to return to the breathing zone.

Increase of ventilation rate plays a significant role in removal of the particles from the domain as well as from the breathing zone. This effect is more prominent in mixed ventilation than displacement ventilation. From Figure 4.10, 4.11, and 4.12 we can observe, where D_{wo}/D_{wp}=1 room with a partition wall), increasing the ventilation rate from ACH 3 to ACH 7 removes ≈15% particles from the room in ceiling ventilation (h_I/h_O=1) and ≈70% in mixed cross ventilation (h_I/h_O>1). When, D_{wo}/D_{wp}=1, ceiling ventilation (Case 9, h_I/h_O=1) has ≈65% less particle in the total domain than displacement ventilation (Case 15, h_I/h_O<1) possessing ≈55% more particles in the breathing zone.

To analyze the flow pattern of the particles we need to study the trajectory over time. In case 15 (D_{wo}/D_{wp}=1 h_I/h_O<1), the particles remain in the exhale zone in clustered form (Figures 4.17(a, b)). From Figure 4.14(c, d), we can infer as the air circulated the room particles trapped in the vortex do not exit the domain and returns to the breathing zone. So, when at ≈ 200s the number got a peak of ≈ 90% particles (Figure 4.13c). On the other hand, for mixed cross ventilation (case 9, D_{wo}/D_{wp}=1, h_I/h_O<1), after reaching a peak at ≈100s with 80% particles in the breathing zone the concentration gradually decreased to ≈9% at 300 s (Figure 4.13c).

After ≈100s the particles started to disperse and move to the inhale zone (Figures 4.13a, b), and travel below the breathing level (Figures 4.13 c, d). That indicated the particles proceeds to the outlet and ensured maximum removal of the particles from the domain as well as from the breathing zone. For the cases where $D_{wo}/D_{wp}<1$(room with a partition wall and desk), ceiling ventilation (case 6, $h_I/h_O=1$) is more efficient with ACH 7 than cross ventilation (case 12 and case 18). Increasing ACH from 3-7 results in removal of the the particles up to ≈ 75% in ceiling ventilation ($h_I/h_O=1$), ≈ 30% in displacement ventilation ($h_I/h_O<1$), ≈ 15% in mixed cross ventilation ($h_I/h_O>1$). In case 6 ($D_{wo}/D_{wp}<1$, $h_I/h_O=1$), the particles disperse and move to the inhale portion (Figure 4.15) that cause removal of particles from the domain as explained in Figure 4.14c where we can see that after ≈100s the particle number gradually decreased from ≈80% to ≈4% at 300s.

To ascertain if there is a change in the particle transport if the diameter is varied i.e. to assess whether airflow velocity dominates the trajectory pattern over the deposition velocity, particles of different diameters, 0.3, 1, 3, 7, and 10 μm, were released. A total of 150,000 particles were released with the same number of particles for each size. Figure 4.18(a) shows that there was negligible influence on the temporal change of the particle number in the breathing zone. Figure 4.18(b) is a snap shot of the spatial distribution of the particles at the end of a simulation for DV, ACH 7 in a room with two desk and a partition. All the particles having the same trajectory indicates dominating influence of the air flow velocity. Particles of the same size appear to cluster and it appears that the size of the particle has minimal effect on particle distribution (Figure 4.19). Exposure to occupant may occur only for a short period of time.

The investigation of the cases shows that while increased ventilation has positive effects both in air quality and particle removal perspective, it alone is not enough and other aspects have to be considered for efficient and economical maintenance of

indoor air quality. For the room with a partition wall only ($D_{wo}/D_{wp} = 1$), increased ventilation makes the ceiling ventilation more effective than the other two types of ventilation patterns. The presence of furniture has significant effect on the velocity profile that influences the particle transport and condition over time. For our problem scenario, we can infer that mixed ventilation with ACH 7 (case 9) appears to be more acceptable ventilation system offering better indoor environment. Although mixed cross ventilation with ACH 3 (case 7) shows slightly less particles in the breathing zone than ACH 5 (case 8), the total particles stays in the room is 100% for both cases. The air flow is in better condition in case 8. And for a room with partition wall and desks, ceiling ventilation with ACH 7 (Case 6) can be identified as better option to provide improved indoor condition. Mixed ventilation with ACH 3 (case 10) seems to be the weakest condition among all the cases.

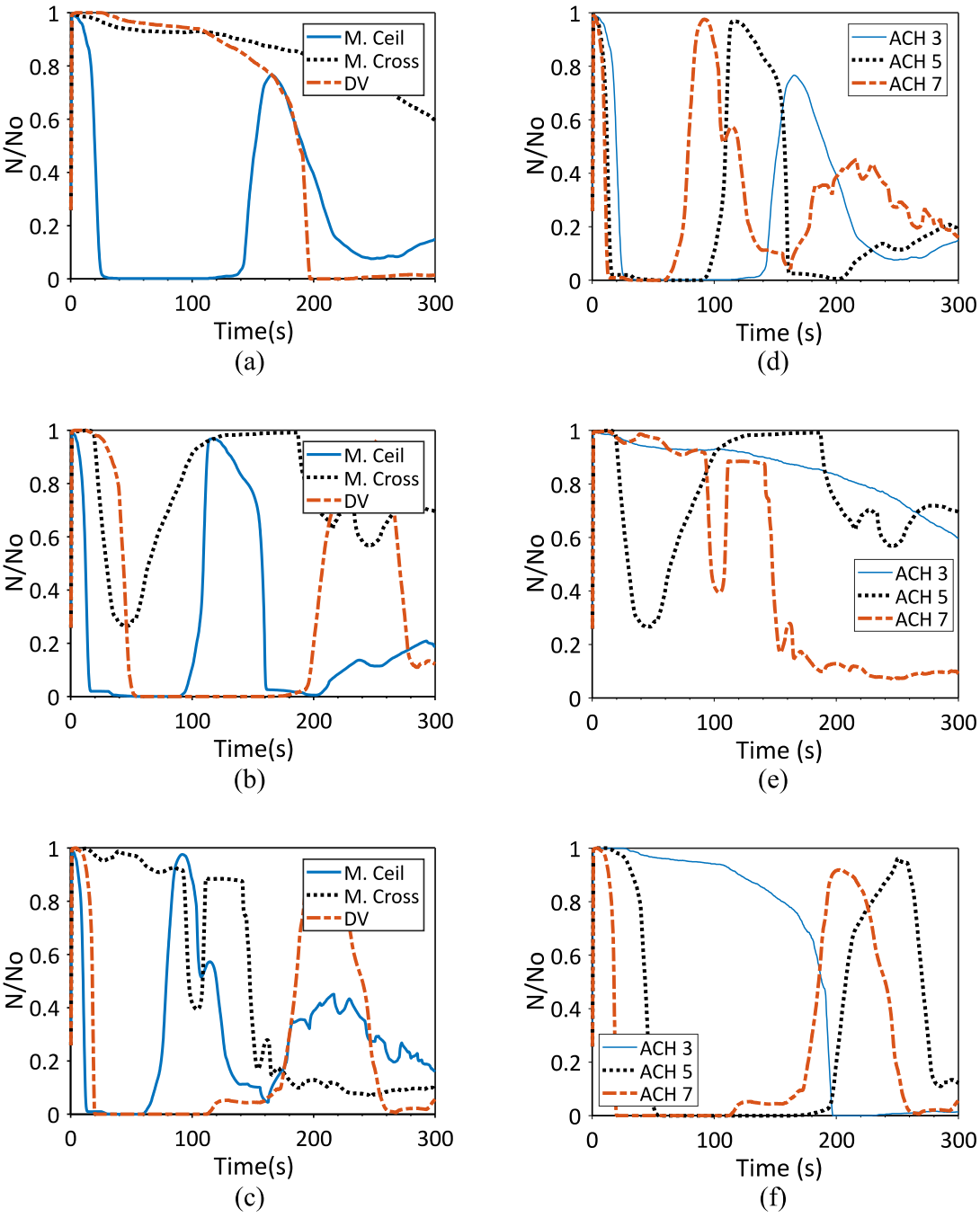

Figure 4.13 Particle in the breathing zone over time, where D_{wo}/D_{wp}=1. a) Effect of ventilation pattern with ACH 3, b) Effect of ventilation pattern with ACH 5, c) Effect of ventilation pattern with ACH 7. d) Effect of ACH in MV. ceiling ventilation, e) Effect of ACH in MV. cross ventilation, f) Effect of ACH in DV. cross ventilation.

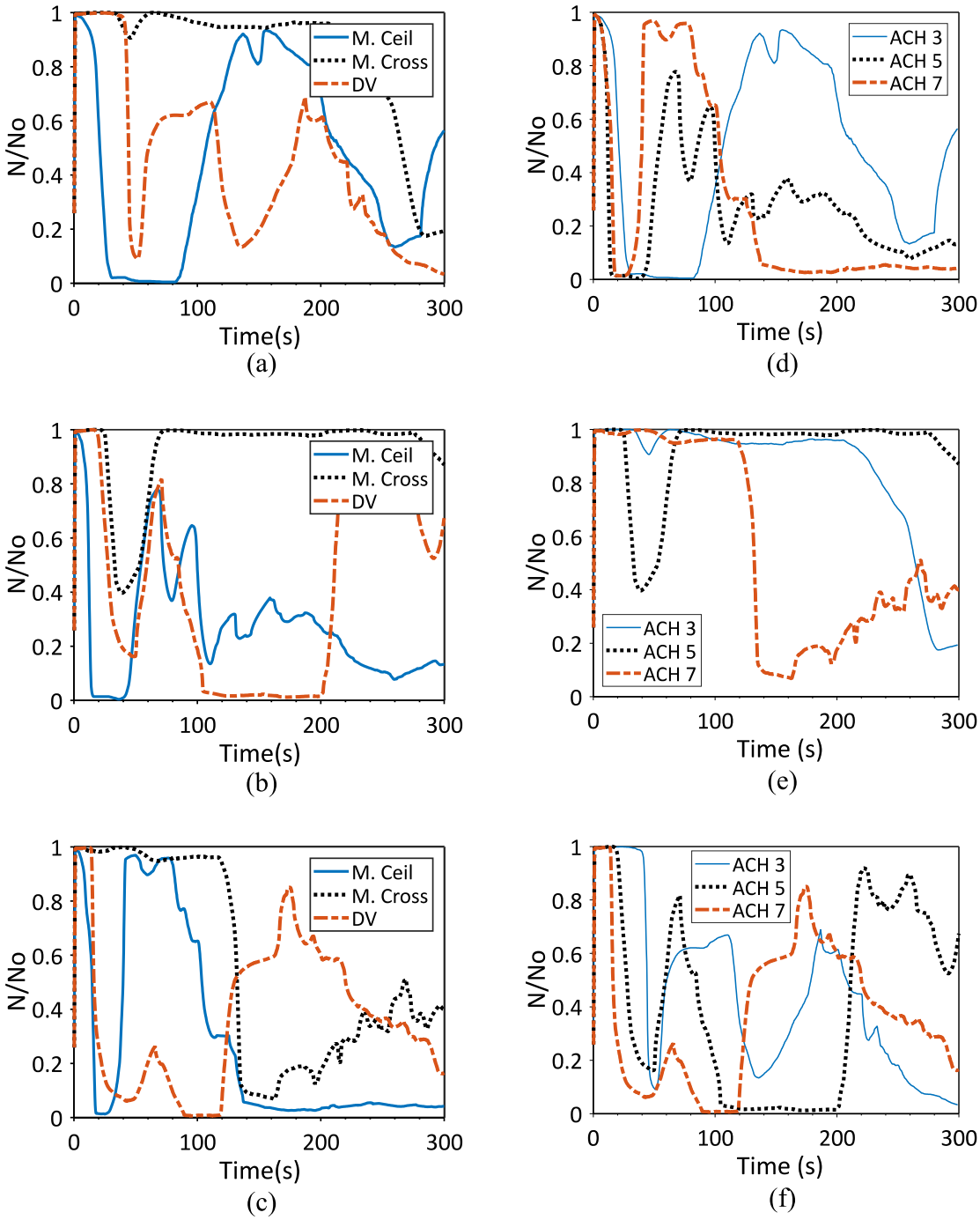

Figure 4.14 Particle in the breathing zone over time, where $D_{wo}/D_{wp}<1$ a) effect of ventilation pattern with ACH 3, b) effect of ventilation pattern with ACH 5, c) effect of ventilation pattern with ACH 7, d) effect of ACH in MV. ceiling ventilation, e) effect of ACH in MV. cross ventilation, f) effect of ACH in DV. cross ventilation.

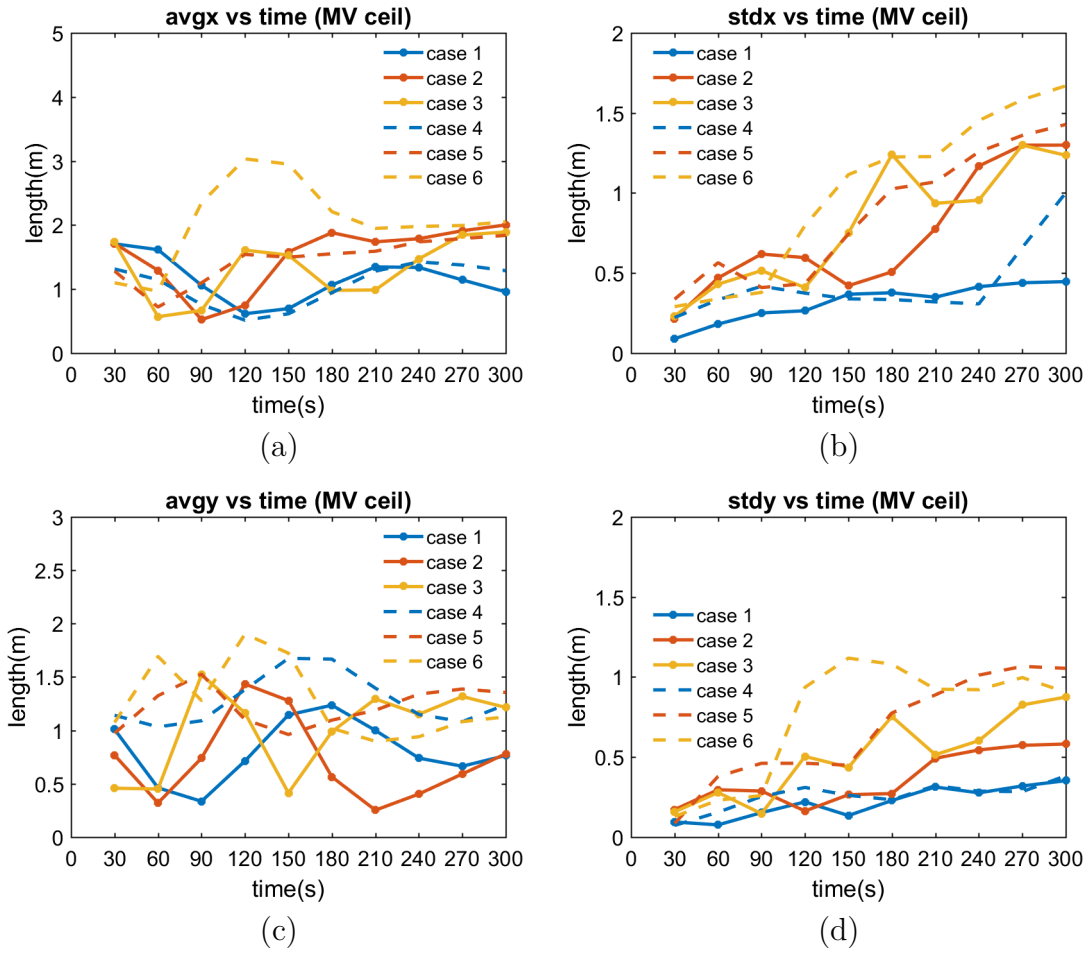

Figure 4.15 Average (a) and standard deviation (b) of x-coordinates, average (c) and standard deviation (b) of y-coordinates of the particles' position over time in the domain for MV Ceil.

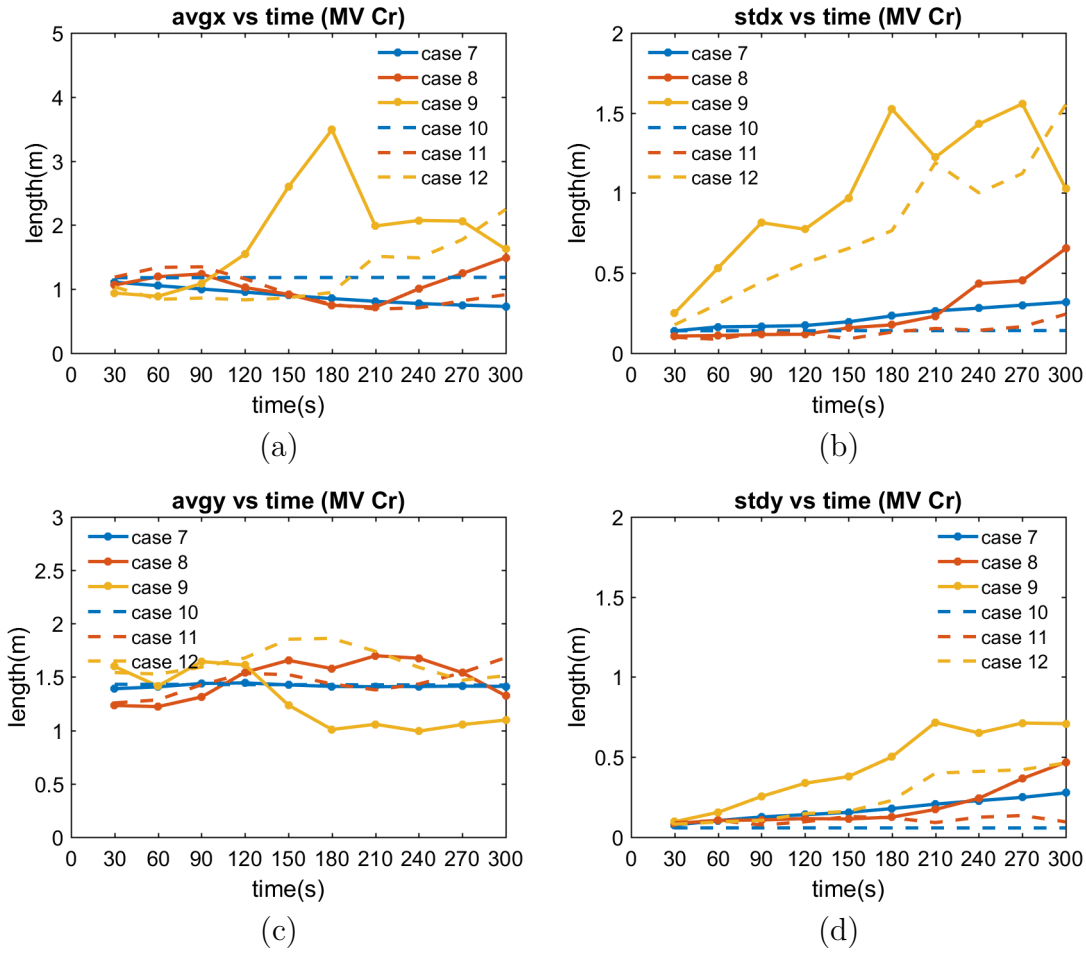

Figure 4.16 Average (a) and standard deviation (b) of x-coordinates, average (c) and standard deviation (b) of y-coordinates of the particles' position over time in the domain for MV Cross.

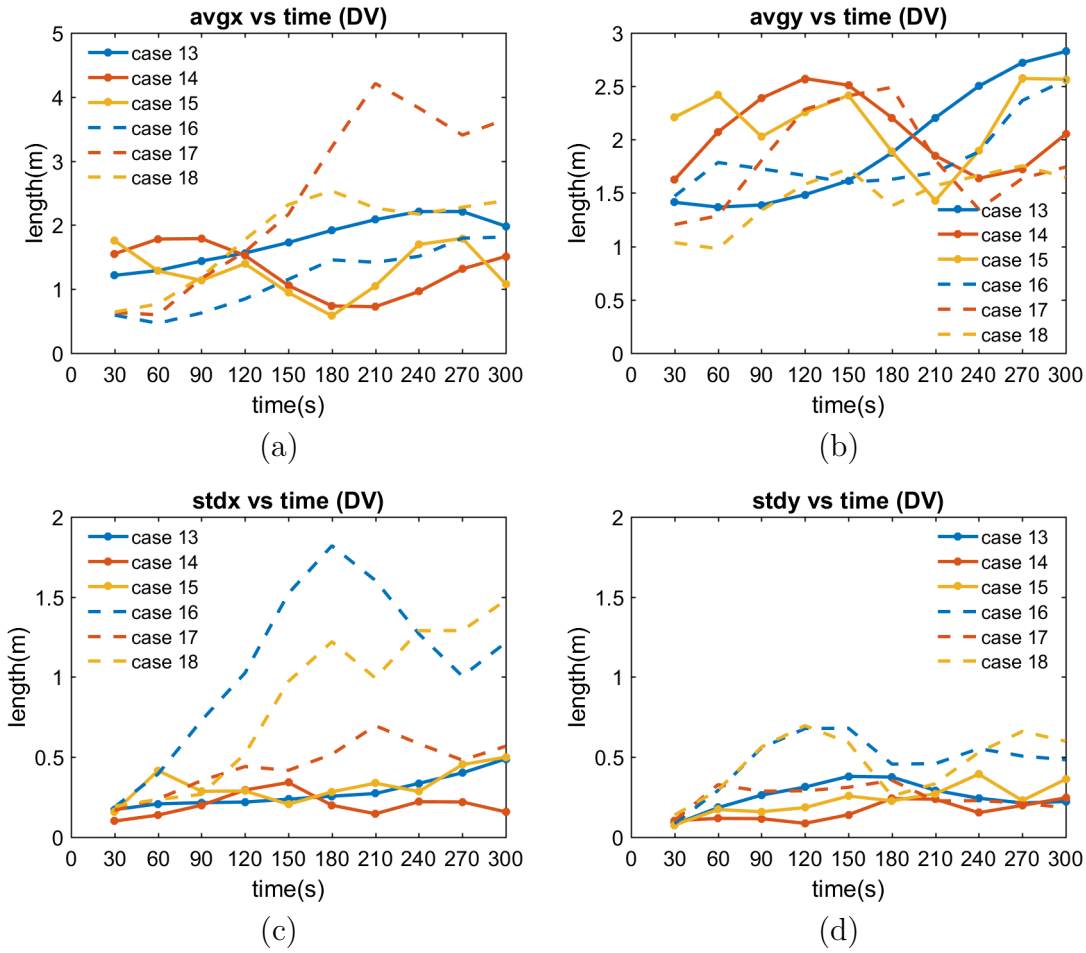

Figure 4.17 Average (a) and standard deviation (b) of x-coordinates, average (c) and standard deviation (b) of y-coordinates of the particles' position over time in the domain for DV.

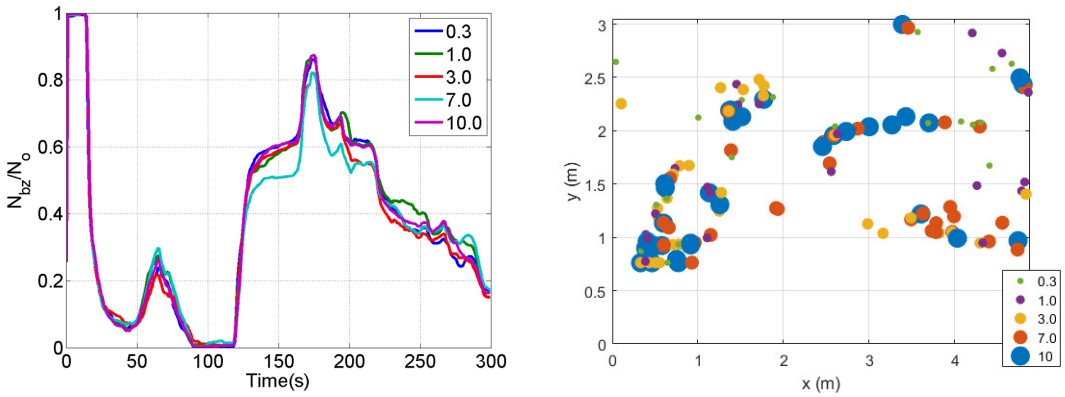

(a) (b)

Figure 4.18 Temporal evolution (a) and spatial distribution (b) of multiple sized particles after 5 min. under DV and ACH 7 in a room with partition and desks.

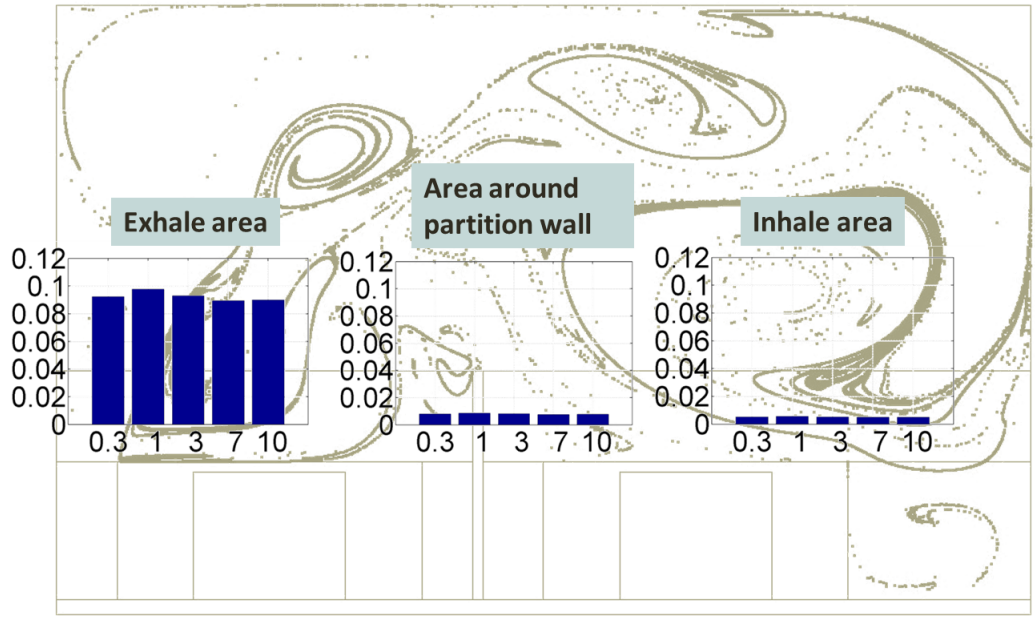

Figure 4.19 Histogram of multiple sized particles' range in different location in a room with furniture having DV cross Ventilation with ACH 7.

Chapter 5

Conclusion and Future Works

5.1 Conclusion

Respiratory aerosols transmit pathogens and can travel short to long range from the source becoming a possible source of infection for the people in range. A cough or sneeze of a flu sufferer can be a vital source of spreading infectious particles among the occupants sharing the space. An indoor environment designed with prior knowledge on how interior design and HVAC parameters influence infection transfer can reduce the risk of spreading infection in a working space without increasing economic costs. A healthy indoor space can be defined as a well-ventilated space having less infectious particle in the room particularly in the breathing zone. In this study, the CFD investigations of air flow and particle behavior in breathing zone and the possibility of transmission between occupants reveal an interacting influence of ventilation type, air changes and aerosol pattern.

Adjusting the ventilation pattern as well as ACH appeared to have a more efficient in removing particles from the room as well as from the breathing zone . For the room with a partition wall only, increasing ACH is more appropriate with mixed cross ventilation pattern. For Mixed cross ventilation, increasing the ACH from 3 to 7 resulted in ≈65% dead zone reduction and also offers reduction of the particles in the breathing zone from 60% to 9% and is more effective to remove the particles from the room. While mixed ceiling ventilation removes ≈ 25% and displacement ventilation removes only about 3% particles, mixed cross ventilation removes ≈70%

of particles from the room while operated with ACH 7. At ACH 7, in a room with a partition wall only, the ventilation pattern has less impact on the air flow. The non-stagnant zone are 75%, 80% and 77% for MV-ceiling, MV-cross and DV respectively. The presence of desks increases the dead zone ratio in MV-ceiling ventilation, while for MV-cross and DV-cross it reduces.

Increasing ACH resulted in increased dead zone for ventilation pattern. Increasing ventilation rate from ACH 3 to 7, the dead zone reduction is ≈42% for MV-ceiling, while ≈ 35% for MV-cross and DV. With ACH 7, introducing furniture rises dead zone by ≈20% in MV ceiling and by ≈50% in MV-cross in total domain.

Presence of furniture plays a role in removing the particles from the room at higher ACH with MV-ceiling and displacement ventilation. In the cross ventilation (both mixed and displacement), the stagnant pockets near and around the desks increase the possibility in trapping the particles in the breathing zone. The particles number in the breathing zone rises from 9% to 40% in MV. cross ventilation and from ≈6% to ≈17% in displacement ventilation.

While MV. ceiling ventilation shows in ACH 7, introduction desks reduces ≈70% particles from the total domain and ≈75% particles from the breathing zone. It was observed that the number of particles present in the breathing zone was governed more by the air circulation and the particles trapped within the vortex.

This study suggests that MV ceiling offers more favorable condition than other ventilation patterns when operating ACH 7. In a room with a partition wall, mixed cross ventilation the particle removal from the room is ≈65% more than mixed-ceiling ventilation and ≈67% more than displacement ventilation when ventilation rate is ACH 7. On the other hand, in the room with a partition wall and the desks, mixed ceiling ventilation removes ≈75% more particles than mixed-cross ventilation and ≈64% more than displacement ventilation with ACH 7. At lower ACH the removal of particle from the room is almost null.

From the study with the average location of the particles over time, we can infer that at lower ACH, mixed ventilation trap the particles in the exhale area and the particles return in the breathing zone in a periodic circulation, while displacement ventilation offers more dispersion of the particles. A preliminary analysis of the influence of particle diameter showed that particle number in the breathing zone did not vary substantially over time when the particles of multiple diameters were released (0.3, 1.0, 3, 7, and 10 μm).

5.2 Future Work

The present study investigates the impact of ventilation, air change and furniture to the transportation of infectious particles and air quality of the space through 2D simulations. A more detailed outlook can be achieved by modeling the situation in 3D, which will ensure better understanding on the displacement ventilation. The data presented in this research are based on numerical analysis. These can be experimentally confirmed by performing lab experiments recreating a full-scale or small scaled scenario. The experiments can be extended varying the partition wall height, furniture locations and internal spacing among them to regulate interior design to achieve a safer and healthier indoor work space.

In this study the infectious particles have been considered to have diameters of 10 micron or less which are appropriate to be modeled as aerosols. The transportation behavior of larger particles (>10 μm) can be affected by gravitational force and large droplet dynamics (Chao et al., 2008; Chen et al., 2010). Exploring the cases with that larger particles can offer more detailed observations of particle transmission in indoor space. In addition, the dispersion of bioaerosols and spread of infections can be investigated more accurately by incorporating the life span and disease transmission mechanisms of the infectious viruses and bacteria. Temperature, humidity, and influence of evaporation will be considered for the later simulations.

Moreover, this research assumed that the occupants are stationary, and both are in seating position. In reality, the occupants do move and can be in sitting and standing position. The impact of occupants' positions and locations can be incorporated as a stochastic disturbance to the flow field.

Bibliography

Afroz, Z., Shafiullah, G., Urmee, T., and Higgins, G. (2018). Modeling techniques used in building HVAC control systems: A review. *Renewable and Sustainable Energy Reviews*, 83(3):64–84.

Ansaripour, M., Abdolzadeh, M., and Sargazizadeh, S. (2016). Computational modeling of particle transport and distribution emitted from a laserjet printer in a ventilated room with different ventilation configurations. *Applied Thermal Engineering*, 103:920–933.

ASHRAE (2016). ANSI/ASHRAE Standard 62.1-2016: Ventilation for acceptable indoor air quality. `https://www.ashrae.org/technical-resources/bookstore/standards-62-1-62-2`.

Basarir, M. N. (2009). Numerical study of the airflow and temperature distributions in an atrium. Master's thesis, Queens University.

Canha, N., Lage, J., Candeias, S., Alves, C., and Almeida, S. M. (2017). Indoor air quality during sleep under different ventilation patterns. *Atmospheric Pollution Research*, 8(6):1132–1142.

Cao, G., Awbi, H., Yao, R., Fan, Y., Sirén, K., Kosonen, R., and Zhang, J. J. (2014). A review of the performance of different ventilation and airflow distribution systems in buildings. *Building and Environment*, 73:171–186.

Chang, T.-J., Hsieh, Y.-F., and Kao, H.-M. (2006). Numerical investigation of airflow pattern and particulate matter transport in naturally ventilated multi-room buildings. *Indoor Air*, 16(2):136–152.

Chao, C. Y. H., Wan, M., and Sze To, G. (2008). Transport and removal of expiratory droplets in hospital ward environment. *Aerosol Science and Technology*, 42(5):377–394.

Chen, C., Zhao, B., Cui, W., Dong, L., An, N., and Ouyang, X. (2010). The effectiveness of an air cleaner in controlling droplet/aerosol particle dispersion emitted from a patient's mouth in the indoor environment of dental clinics. *Journal of the*

Royal Society Interface, 48(7):1105–1118.

Cole, E. C. and Cook, C. E. (1998). Characterization of infectious aerosols in health care facilities: an aid to effective engineering controls and preventive strategies. *American journal of infection control*, 26(4):453–464.

EPA (2003). Volatile Compounds' Impact on Indoor Air Quality. `https://www.epa.gov/indoor-air-quality-iaq/volatile-organic-compounds-impact-indoor-air-quality`.

ESI (2014). CFD-ACE+. `https://www.esi-group.com/software-solutions/virtual-environment/cfd-multiphysics/ace-suite/cfd-ace`.

Faulkner, W. B., Memarzadeh, F., Riskowski, G., Kalbasi, A., and Ching-Zu Chang, A. (2015). Effects of air exchange rate, particle size and injection place on particle concentrations within a reduced-scale room. *Building and Environment*, 92:246–255.

Gao, N. and Niu, J. (2007). Modeling particle dispersion and deposition in indoor environments. *Atmospheric Environment*, 41(18):3862–3876.

Hathway, E., Noakes, C., Sleigh, P., and Fletcher, L. (2011). CFD simulation of airborne pathogen transport due to human activities. *Building and Environment*, 46(12):2500–2511.

Hoque, S., Farouk, B., and Haas, C. N. (2009). Multiple linear regression model approach for aerosol dispersion in ventilated spaces using computational fluid dynamics and dimensional analysis. *Journal of Environmental Engineering*, 136(6):638–649.

Keech, M. and Beardsworth, P. (2008). The impact of influenza on working days lost. *Pharmacoeconomics*, 26(11):911–924.

Klepeis, N. E., Nelson, W. C., Ott, W. R., Robinson, J. P., Tsang, A. M., Switzer, P., Behar, J. V., Hern, S. C., and Engelmann, W. H. (2001). The National Human Activity Pattern Survey (NHAPS): a resource for assessing exposure to environmental pollutants. *Journal of Exposure Science and Environmental Epidemiology*, 11(3):231.

Knudsen, S. M., Gunnarsen, L., and Madsen, A. M. (2017). Airborne fungal species associated with mouldy and non-mouldy buildings–effects of air change rates, hu-

midity, and air velocity. *Building and Environment*, 122:161–170.

Lindsley, W. G., Pearce, T. A., Hudnall, J. B., Davis, K. A., Davis, S. M., Fisher, M. A., Khakoo, R., Palmer, J. E., Clark, K. E., Celik, I., et al. (2012). Quantity and size distribution of cough-generated aerosol particles produced by influenza patients during and after illness. *Journal of occupational and environmental hygiene*, 9(7):443–449.

Liu, S. and Novoselac, A. (2014). Transport of airborne particles from an unobstructed cough jet. *Aerosol Science and Technology*, 48(11):1183–1194.

Liu, W., Liu, D., and Gao, N. (2017). CFD study on gaseous pollutant transmission characteristics under different ventilation strategies in a typical chemical laboratory. *Building and Environment*, 126:238–251.

Lu, W. and Howarth, A. T. (1996). Numerical analysis of indoor aerosol particle deposition and distribution in two-zone ventilation system. *Building and Environment*, 31(1):41–50.

Lu, W., Howarth, A. T., Adam, N., and Riffat, S. B. (1996). Modelling and measurement of airflow and aerosol particle distribution in a ventilated two-zone chamber. *Building and Environment*, 31(5):417–423.

Memarzadeh, F. and Xu, W. (2012). Role of air changes per hour (ACH) in possible transmission of airborne infections. *Building Simulation*, 5(1):15–28.

Morawska, L. (2006). Droplet fate in indoor environments, or can we prevent the spread of infection? *Indoor Air*, 16(5):335–347.

Nicas, M., Nazaroff, W. W., and Hubbard, A. (2005). Toward understanding the risk of secondary airborne infection: emission of respirable pathogens. *Journal of occupational and environmental hygiene*, 2(3):143–154.

OSHA (2016). Breathing zone. `https://www.osha.gov/`.

Pejtersen, J. H., Feveile, H., Christensen, K. B., and Burr, H. (2011). Sickness absence associated with shared and open-plan offices—a national cross sectional questionnaire survey. *Scandinavian Journal of Work, Environment & Health*, pages 376–382.

Piomelli, U. (1999). Large-eddy simulation: achievements and challenges. *Progress in Aerospace Sciences*, 35(4):335–362.

Posner, J., Buchanan, C., and Dunn-Rankin, D. (2003). Measurement and prediction of indoor air flow in a model room. *Energy and buildings*, 35(5):515–526.

Putra, J. C. P. and Rahman, I. A. (2017). Effects of inlet air supply on particle deposition in an office building. *Procedia Engineering*, 170:189–194.

Quang, T. N., He, C., Morawska, L., and Knibbs, L. D. (2013). Influence of ventilation and filtration on indoor particle concentrations in urban office buildings. *Atmospheric Environment*, 79:41–52.

Roache, P. J. (1994). Perspective: a method for uniform reporting of grid refinement studies. *Journal of Fluids Engineering*, 116(3):405–413.

Roache, P. J. (1997). Quantification of uncertainty in computational fluid dynamics. *Annual review of fluid Mechanics*, 29(1):123–160.

Sørensen, D. N. and Nielsen, P. V. (2003). Quality control of computational fluid dynamics in indoor environments. *Indoor air*, 13(1):2–17.

Staples (2016). The impact of flu on workplace productivity: Insights from Staples sixth annual flu survey. `https://www.staplesadvantage.com/sites/health-wellness/executive-summary.html`.

Sundell, J., Levin, H., Nazaroff, W. W., Cain, W. S., Fisk, W. J., Grimsrud, D. T., Gyntelberg, F., Li, Y., Persily, A., Pickering, A., et al. (2011). Ventilation rates and health: multidisciplinary review of the scientific literature. *Indoor Air*, 21(3):191–204.

Thatcher, T. L., Lai, A. C., Moreno-Jackson, R., Sextro, R. G., and Nazaroff, W. W. (2002). Effects of room furnishings and air speed on particle deposition rates indoors. *Atmospheric Environment*, 36(11):1811–1819.

Tian, Z., Tu, J., and Yeoh, G. (2007). CFD studies of indoor airflow and contaminant particle transportation. *Particulate Science and Technology*, 25(6):555–570.

Toolbox, E. (2005). Air change rates in typical rooms and buildings. `https://www.engineeringtoolbox.com/air-change-rate-room-d_867.html`.

Wargocki, P., Wyon, D. P., Sundell, J., Clausen, G., and Fanger, P. (2000). The effects of outdoor air supply rate in an office on perceived air quality, sick building syndrome (SBS) symptoms and productivity. *Indoor Air*, 10(4):222–236.

Wu, W., Skye, H. M., and Domanski, P. A. (2018). Selecting HVAC systems to achieve comfortable and cost-effective residential net-zero energy buildings. *Applied Energy*, 212:577–591.

Xu, J. and Pope, S. B. (2000). Pdf calculations of turbulent nonpremixed flames with local extinction. *Combustion and Flame*, 123(3):281–307.

Yang, S., Lee, G. W., Chen, C.-M., Wu, C.-C., and Yu, K.-P. (2007). The size and concentration of droplets generated by coughing in human subjects. *Journal of Aerosol Medicine*, 20(4):484–494.

Zhou, Y., Deng, Y., Wu, P., and Cao, S.-J. (2017). The effects of ventilation and floor heating systems on the dispersion and deposition of fine particles in an enclosed environment. *Building and Environment*, 125:192–205.

Zhu, S., Kato, S., and Yang, J.-H. (2006). Study on transport characteristics of saliva droplets produced by coughing in a calm indoor environment. *Building and Environment*, 41(12):1691–1702.